Reverse Lipofection for Spatially Defined Transfection with DNA/Cationic Lipoplexes

Ana Inês Botelho de Gomes Meleiro

Thesis to obtain the Master of Science Degree in

Biotechnology

Supervisors: Professor Gabriel António Amaro Monteiro

Doctor Fábio Monteiro Fernandes

Examination Committee

Chairperson: Professor Arsénio do Carmo Sales Mendes Fialho

Supervisor: Doctor Fábio Monteiro Fernandes

Members of the Committee: Professor Marília Clemente Velez Mateus

December 2015

I. ACKNOWLEDGEMENTS

I would like to thank both my supervisors, Professor Gabriel Monteiro and Doctor Fábio Fernandes for accepting me as their student. For me, the main goal of a master thesis was always to learn and by giving me the opportunity to develop this method I had the chance to learn several techniques and learn about different areas of expertise. For this, and for the constant help and support, I thank you.

I also would like to thank several people without whom this work wouldn't be possible:

- Sandra Pinto
- Salomé Magalhães
- Prof. Ana Azevedo
- Nuno Bernardes and Dalila Mil-Homens
- Maria João Sarmento, Joana Serra and Diogo Silva
- iBB and CQFM colleagues
- Friends and above all to my Family.

II. RESUMO

Apesar de as terapias génicas serem consideradas para fins terapêuticos, a entrada do gene no núcleo é a maior barreira a uma eficiente transfeção celular. Em detrimento do uso de métodos virais, surgiram os métodos não virais de entrega de genes e o uso de materiais para o empacotamento do ADN tais como lípidos catiónicos são atualmente considerados métodos cruciais para a entrega e proteção dos genes de, por exemplo, nucleases e outras barreiras dentro da célula.

Assim, no presente trabalho propõe-se um novo método de transfeção reversa que poderá combinar as vantagens do uso de lípidos catiónicos com tecnologias de matrizes celulares. Neste novo método, os lipoplexos são imobilizados no substrato, antes da colocação das células, através da ligação avidina-biotina.

Numa primeira abordagem, a imobilização dos lipoplexos foi testada e realizados vários ensaios exploratórios. De seguida, através de Métodos de Superfície de Resposta (MSR), foram variadas cinco variáveis (concentração de lípidos, proporção DOTAP:DOPE, número inicial de células, concentração de pADN e tamanho do lipossoma) conhecidas por influenciar a eficiência de transfeção. Desta forma, não só se obteve o efeito de cada variável como também o efeito da interação entre variáveis na eficiência de transfeção.

Obteve-se uma transfeção máxima de 63,3% e observou-se que a proporção DOTAP:DOPE e a concentração de lípido foram as variáveis com mais efeito na eficiência transfeção. Apesar de se concluir que a região experimental sob estudo estava deslocada da região ideal para uma transfeção ótima, experiências futuras poderão ser desenhadas através das conclusões aqui retiradas.

Palavras-chave: transfeção reversa, lípidos catiónicos, imobilização de lipoplexos, MSR, concentração de lípidos, proporção DOTAP:DOPE

III. ABSTRACT

Although gene therapies shown considerable promise for therapeutic purposes, gene nuclear delivery is still a major bottleneck for efficient cellular transfection. Over viral gene delivery, non-viral methods have emerged and the use of DNA packing materials such as cationic lipids, are now considered crucial methodologies to deliver and protect the gene from DNAses and other barriers once inside the cells.

To this end, we propose a new reverse transfection methodology that is likely to allow the combination of cell array technologies with the advantages of cationic lipid-based gene delivery. In this new method, lipoplexes are immobilized onto the substrate taking advantage of the ligation avidin-biotin before cell plating.

In a first approach, the immobilization of lipoplexes was tested and some exploratory assays were performed. Secondly and by means of Response Surface Methodologies (RSM) five variables (lipid concentration, DOTAP:DOPE proportion, initial number of cells, pDNA concentration and liposome size) known to influence transfection efficiency were allowed to vary. In this way, not only the effect of each variable was obtained but also the effect of the interaction between variables in the response variable.

A maximum 63.3% transfection efficiency was obtained and DOTAP:DOPE proportion and Lipid Concentration were observed to be the variables that have the most significant effect on transfection efficiency. Although it was concluded that the experimental region under study was far from the ideal region for an optimum transfection, further experiments can be drawn from the conclusions here taken.

Keywords: reverse transfection, cationic lipids, lipoplexes immobilization, RSM, lipid concentration, DOTAP:DOPE proportion

IV. TABLE OF CONTENTS

V. LIST OF FIGURES

VI. LIST OF TABLES

VII. ABBREVIATIONS

AFM – Atomic Force Microscopy

ANOVA – Analysis Of Variance

BAM modified glass slides - Biocompatible Anchor for Membrane modified glass slides

CCD – Central Composite Design

CCF – Face Centered Central Composite design

cDNA – complementary DNA

Chol – Cholesterol

CMV – Cytomegalovirus Immediate Early Promoter

CTAB – cetyltrimethylammonium bromide

dF – Degrees of Freedom

DMEM - Dulbecco's Modified Eagle Medium

DMSO - Dimethyl Sulphoxide

DNA – Deoxyribonucleic acid

DOGS – dioctadecylamidoglycylspermine

DOPC – 1,2-dioleoyl-*sn*-glycero-3-phosphocholine

DOPE – 1,2-dioleoyl-*sn*-glycero-3-phosphoethanolamine

DOPE-Cap-biotin - 1,2-dioleoyl-*sn*-glycero-3-phosphoethanolamine-N-(cap biotinyl)

DOPE-Rho – ,1,2-dioleoyl-*sn*-glycero-3-phosphoethanolamine-N-(lissamine rhodamine B sulfonyl)

DOSPA-1,3-dioleoyloxy-N-[2-(sperminecarboxamido)ethyl]-N,N-dimethyl-1-propanaminium trifluoroacetat

DOTAP - 1,2-dioleoyloxy-3-trimethylammonium propane

DOTMA – N-[1-(2,3-dioleyloxy) propyl]-N,N,N-tri-methylammoniumchloride

E. coli – *Escherichia coli*

EDTA - Ethylenediaminetetraacetic acid

EVAC polymer – Ethylene vinyl acetate polymer

FBS – Fetal Bovine Serum

FSC – Forward Scatter

GC – Gold Colloidal

gDNA – Genomic DNA

GFP – Green Fluorescent Protein

HEK 293T – Human Embryonic Kidney 293T cell line

Hic-Sec – Hydrophobic Interaction Size Exclusion Chromatography

H^{II}_{C} – inverted hexagonal structure

HIV – Human Immunodeficiency Virus

hMSC's – human Mesenchymal Stem Cells

IgA – Immunoglobulin A

LB – Luria Bertani

L^{C}_{α} – lamelar structure

LOF – Lack of Fit

LUV – Large Unilamellar Vesicle

MS – Mean Square

NLS – Nuclear Localization Signal

OD – Optical Density

PAMAM – Polyamidoamine

PBS – Phosphate Buffer Solution

pDNA – Plasmid DNA

PEI – Polyethylenimine

PES – Polyethersulfone

PFA – Paraformaldehyde

PLL – Poly-L-Lysine

RNA – Ribonucleic Acid

RSM – Response Surface Methodologies

SLB – Supported Lipid Bilayer

SS – Sum of Squares

SSC – Side Scatter

SUV – Small Unilamelar Vesicle

TAE – Tris-Acetate-EDTA

TAT – Trans-Activating Transcriptional Activators

Ti:Sa – Titanium:Saphire

SV40 - Simian Vacuolating Virus 40

WERI-Rb1 cell line – retinoblastoma cell line

1. INTRODUCTION

Gene therapy is used to transfer genetic material to specific cells with a therapeutic purpose. It can be used for gene insertion, gene compensation or to produce a beneficial protein[1]. But efficient nuclear delivery of genes remains a major bottleneck for gene therapy methods. Furthermore, introducing DNA into cells is a crucial method for basic science studies on gene function, metabolic and signaling pathways, cytotoxicity, drug delivery, etc. Recently, cell array techniques have been used in combination with gene delivery technologies to increase the reproducibility and to increase data output [2].

Although there are several developed methods for transfection, there is still a major difference between what is applied *in vitro* versus what can be applied *in vivo* including in human therapeutic applications. Therefore, significant efforts are currently in place in this field towards new gene delivery methodologies.

When it comes to choosing a gene delivery method, there are 3 major aspects that have to be taken into account. Firstly, it has to protect the transgene from the action of nucleases inside the cell. Secondly, in order for the gene to be expressed it has to pass through the nuclear envelope. Lastly, it can´t have any cytotoxicity or have other negative effects on the cell physiology [3]. In an ultimate analysis, any transfection method should be reproducible and easy to use.

1.1. Gene Delivery Methods

Gene delivery methodologies can be divided into two main components: the transgene vector, which can be a viral vector or plasmid DNA (pDNA) (non-viral vector) and its vehicle.

1.1.1.Transgene Vector

Viral vectors as the name indicates uses viruses and are the most used method for clinical research mainly for cancer diseases[4]. Their high applicability and efficiency is based on the principle that viruses are able to integrate in the host genome, but this is also one of the major drawbacks of this technology [5]. Because of its virus nature, the transgene integrates randomly in the host genome and may interrupt essential genes or disrupt tumor suppressor genes[6]. Furthermore, viral vectors also have disadvantages regarding immune recognition[7,8]. Additionally, adenovirus associated virus for example, have proven to be very efficient with both dividing and non-dividing cells and are non-pathogenic but have the drawback of low capacity regarding the size of the transgene (<5kB)[9].
For these reasons non-viral gene delivery has been much explored although viral technologies are more efficient.

Plasmid DNA (pDNA) has being used for therapeutic purposes for more than 20 years. Among its several advantages are the easy manipulation, low cost of production and purification. Also, since the supercoiled isoform used in vaccines is stable, there is no need for expensive store and transportation conditions[10]. Clinical trials with naked or pDNA worldwide account for more than 17% plus its use combined with other technologies. (Figure 1.1)

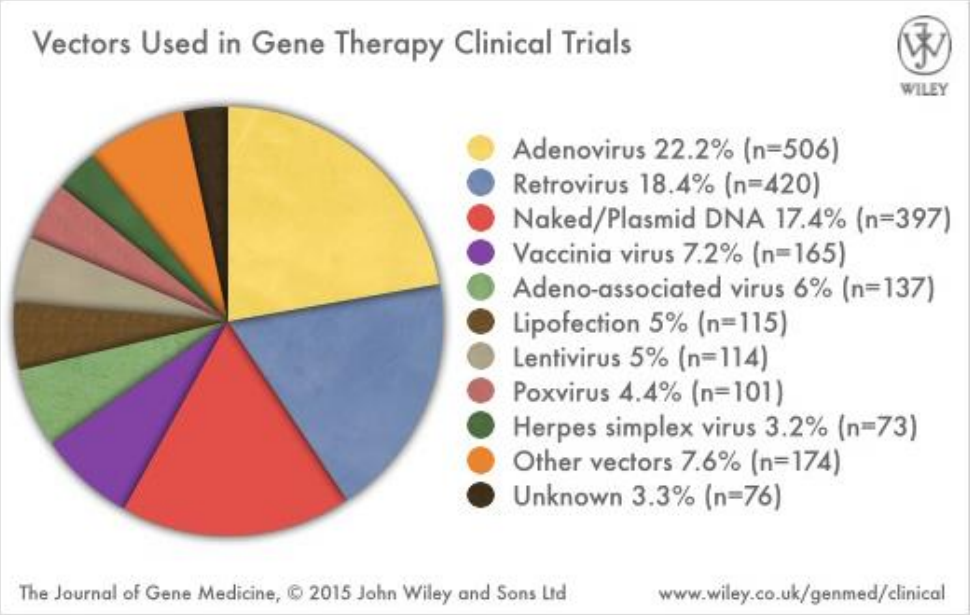

Vector	Gene Therapy Clinical Trials	
	Number	%
Naked/Plasmid DNA	387	17.5
Naked/Plasmid DNA + Adenovirus	3	0.1
Naked/Plasmid DNA + Modified Vaccinia Ankara virus (MVA)	2	0.1
Naked/Plasmid DNA + Vaccinia virus	3	0.1
Naked/Plasmid DNA + Vesicular stomatitis virus	2	0.1

Figure 1.1 - Types of vectors used in clinical trials worldwide. Naked pDNA accounts for more than 17% of the vectors used. The table shows other technologies in which pDNA is used in association with. (Figure adapted from http://www.abedia.com/wiley/vectors.php)

Plasmid DNA used for gene delivery typically contains a bacterial backbone and a portion for eukaryotic expression. Bacterial backbone is essential for plasmid replication inside bacteria and therefore contains a bacterial origin of replication and a gene for selective pressure. For the eukaryotic part, a eukaryotic

promoter is needed, such as the CMV promoter, and normally a polyadenylation signal is also included [10], For gene delivery, plasmids should be in their supercoiled isoform, aiming for maximum stability and reduced size.

Furthermore, other type of DNA molecules, such as minicircles, are being studied for therapeutic purposes. Minicircles are small supercoiled DNA molecules that are devoid the bacterial backbone. This is achieved through an induction of recombination during the production of the parental plasmid between two direct repeats. This originates two different supercoiled DNA molecules, the minicircle and the undesired miniplasmid. Minicircles show increased transfection efficiency and transgene expression when compared to their parental plasmid counterparts[11].

pDNA can be directly injected into a cell using a needle. Its efficiency depends largely on the cell type that is injected and it has been proven to be very efficient in hepatocytes. It has no toxicity since genes are directly injected but have in general low level of gene expression[12]. Therefore, typically other methods are used in association with pDNA to increase gene expression.

1.1.2. Vehicle Method

Gene transfer by gene gun, micro-injection, laser irradiation, electroporation, sonoporation, magnetofection and hydrodynamic gene delivery are examples of vehicle methods for gene delivery[3,13].

Gene gun or biolistic consists of a bombardment of DNA-coated particles into cells. The efficiency of this technique depends on several parameters including the size of the particle and the conditions of the bombardment. Electroporation is a widely used technique where cells are subjected to a transient electric field that causes a destabilization of the cell barriers opening a way for DNA to enter. Sonoporation works in a similar way but instead of having an electric field, cells are subjected to ultrasound. In magnetofection (simple word for magnetic field-enhanced transfection) the magnetic field role is to concentrate iron-oxide DNA coated particles on top of the cells. The magnetic field force help the entrance of the particles in the cell. Viral or non-viral vectors can be used with this technique as well as a combination of other transfection techniques. These techniques are in general efficient but still have the problem of targeting without becoming fastidious and the problem of poor penetration across tissues[13].

Finally, hydrodynamic gene delivery is mainly applied to gene delivery to the mice liver and it relies on the properties of fluids passing through blood vasculature. It works with viral and non-viral vectors[14] .

Furthermore, single cell transfection techniques have been used. These techniques allow the study of single cells as discrete units and showed to be very useful in understanding mechanisms such as the transfection efficiency variation from cell to cell, cell mechanisms during growing and the study of polarized cells [5]. These techniques are performed mainly in three ways: using Atomic Force Microscopy (AFM) tips and nanoneedles[15,16], electroporation with a micropipette full of DNA and electric stimulation[17] and phototransfection using a multi-photon laser.[18] In general, all the techniques have in common the need of a

microscope to be performed. Although one is able to manipulate any type of mammalian cells with these techniques they are still single cell manipulation methods which makes it difficult to apply in a high-throughput manner.

Table 1.1 summarizes the basic principles, advantages and limitations of the techniques referred before.

Table 1.1 Basic principles, advantages and limitations of gene carrier techniques

Technique	Basic Principle	Advantage	Limitation
Viral vectors	Virus nature	Very efficient	Immunogenic and random integration
Chemical packaging	Charges interstatic interaction	DNA protection from degradation	Clearance *in vivo*
Injection	Needle injection	Simple	Low transgene expression
Gene Gun	Particle bombardment		Difficult to apply *in vivo*
Electroporation	Membrane destabilization due to electric field	Efficiency	Cells may not recover from membrane damage
Sonoporation	Membrane destabilization due to ultrasound	Efficiency	Cells may not recover from membrane damage
Magnetofection	Particle direction through magnetic fields	Targeting	
Hydrodynamic Gene Delivery	Hydrodynamic tissue properties	Very efficient in mice hepatocytes	Difficult to use in humans
Single cell techniques	Various	Cell biology studies	Fastidious

Although naked pDNA is able to transfect in vivo, packing pDNA with cationic molecules and other chemicals can facilitate the uptake and the transfection both in vivo and in vitro. These chemicals among others are able to protect DNA inside the cell and prevent its degradation by nucleases and serum components[19]. Moreover, they promote a less negative surface charge and can be tailored with other molecules to promote cell targeting[20]. Therefore, these systems are the most widely studied and are subject of exhaustive investigations to increase its gene delivery efficiency.

Chemical methods for gene complexation and delivery were the first to be introduced on non-viral gene delivery methods. They have in common the transformation of the DNA molecule into a nanoparticle form

to facilitate cell entry. Efficient transfection when using such methods depends mainly on particle size, pH, salt concentrations, interactions with other molecules and ultimately on the target cell type.

Chemical compounds for gene complexation range from cations such as lipids and polymers, to carbohydrates, polypeptides and dendrimers, among others.

Cationic polymers are the oldest chemical gene delivery system studied, although they are not the most applied in clinical trials. Poly-L-Lysine (PLL) and Polyethylenimine (PEI) are among the most widely studied polymers for DNA complexation and gene delivery[21] .

Chitosan is gaining some attention as a carbohydrate polymer for gene delivery. Besides being biocompatible, biodegradable and exhibiting low toxicity, it has proven to be efficient as a gene deliver method[22,23].

Polypeptide vectors are able to deliver small oligonucleotides by using small sequences of basic amino acids that readily cross the plasma membrane. They are usually called cell-penetrating peptides and one example of such peptides are the trans-activating transcriptional activators (TAT). Generally, in peptide-oligonucleotide delivery strategies, the peptide is covalently bond to the oligonucleotide rather than complexed via electrostatic interactions[24].

Polyamidoamine (PAMAM) have become the most applied dendrimer-base vector for gene deliver. Dendrimers consists of a core molecule that act as the root from which a number of highly branched, tree like arms originate in an ordered and symmetric fashion. Their unique molecular architecture offers multiple conjugation sites and their stepwise method of synthesis gives these molecules the characteristic of having a well-defined size and structure [25] .

Additionally, calcium phosphate has also been used as a DNA complexation agent. Gene delivery using calcium phosphate relies on the principle that the divalent Ca^{2+} cation is able to interact with DNA and form a complex. Although this system is efficient, it has some disadvantages due to low stability of the Ca^{2+} crystals [26].

In the next chapter, the use of lipids for gene packing and delivery will be addressed.

1.2. Cationic Lipid Based Gene Delivery

The first report of cationic lipids being use for efficient gene delivery comes from 1987 by Felgner et al[27]. The sources of interest on cationic lipids are the fact that they are very simple to use and synthesize, while showing high transfection rates and presenting relatively low toxicity comparing to other systems [28].

A neutral lipid (so-called helper or fusogenic lipid) is also typically included together with cationic lipids in the lipid mixture[29].

1.2.1.Cationic Lipids

Cationic lipids can be divided into five main groups according to its headgroup: monovalent cationic lipids, polyvalent cationic lipids, guanidine containing compounds, cholesterol derivatives and cationic peptides[30]. They are amphiphiles and their structures are analogous to the natural lipids except for the presence of positively charged groups. They have long hydrocarbon chains, usually two alkyl chains, which gives them their hydrophobic characteristic, while their amphiphilic character is due to the presence of a charged headgroup containing a quaternary ammonium.[31] Upon hydration, cationic lipids self-assemble into lamellar vesicular structures with interior aqueous phase (liposomes). Inverted hexagonal is another structural phase that these lipids may assume that is likely to play an important part in efficient nuclear gene delivery[31,32].

In this section, it is intended to review some characteristics of the commonly used cationic lipids in gene delivery (DOTAP, DOTMA, DOSPA, DOGS, CTAB) by comparing them with the one used in this work, DOTAP.

The most used cationic lipid for gene delivery is 1,2-dioleoyloxy-3-trimethylammonium propane (DOTAP) which is a monovalent cationic lipid. Asides from DOTAP, other similar cationic lipid DOTMA (N-[1-(2,3-dioleyloxy) propyl]-N,N,N-tri-methylammoniumchloride) was the first to be used. It is also a monovalent cationic lipid and they both have two monounsaturated fatty acid chains[33]. In Figure 1.2 both structures are depicted. DOTAP and DOTMA differ in the chemistry of the linker group which may explain their difference in transfection efficiency. While DOTAP has an ester bond which is endogenous to natural lipids, DOTMA has an ether bond[34]. This way DOTMA becomes more susceptible to the action of cellular lipases or esterases that easily degrade the artificial lipid. Therefore, DOTAP shows higher transfection efficiency and less toxicity[34].

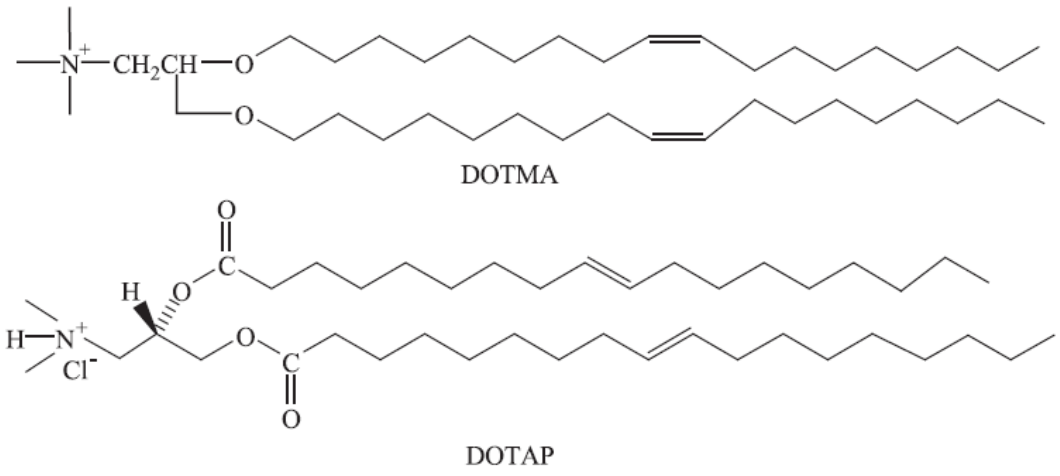

Figure 1.2 Structures of DOTMA and DOTAP. Both share an analogous structure to natural lipids: two monounsaturated fatty acid chains and a hydrophobic charged headgroup which gives them the amphiphilic characteristic. Regarding the chemistry of the linker group (portion that binds the headgroup and the two fatty acid chains) DOTMA has an ether bond and DOTAP has an ester bond. (Figure adapted from Zhang et al, 2004)

Multivalent cationic lipids show a higher capacity to compact DNA than DOTAP. DOSPA (1,3-dioleoyloxy-N-[2-(sperminecarboxamido)ethyl]-N,N-dimethyl-1-propanaminium trifluoroacetat) and DOGS (dioctadecylamidoglycylspermine) are examples of such lipids and they form micellar structures instead of vesicular ones[35]. Although they have proven to be more efficient in DNA complexation, this doesn't necessary translate into better transfection efficiencies, since the intracellular DNA dissociation from these lipids tend to be more difficult[36].

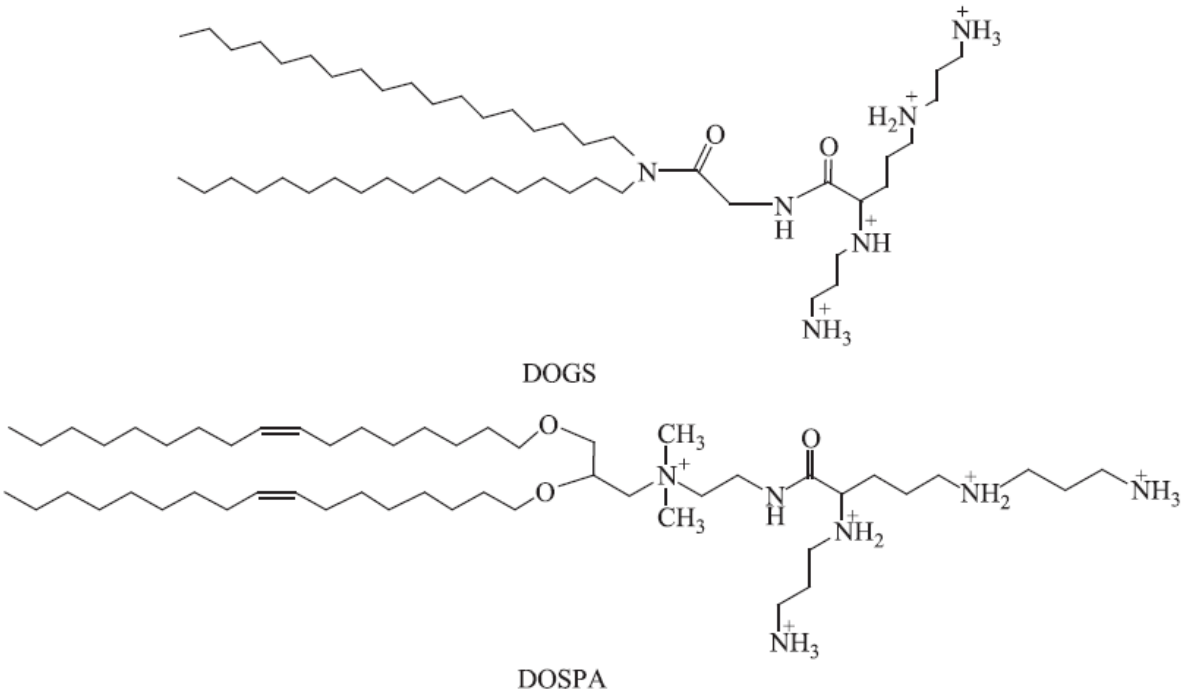

Figure 1.3 Structures of DOGS and DOSPA. Notice the difference in the number of cationic groups present in the headgroup

Cationic lipids may have three different types of hydrophobic domains: aliphatic chains, steroid hydrophobic domains and fluorinated hydrophobic domains. Since the cationic lipid used in this work, DOTAP, has two aliphatic chains, the latter two types won´t be addressed. It is also possible to find cationic lipids used in transfection with 1-4 aliphatic chains. Regarding the size of the alkyl and saturation of the chains, in general increasing the alkyl chain and saturation of a cationic lipid decreases the transfection efficiency. Shorter alkyl chain length favors higher rates of intermembrane transfer of lipid monomers and lipid membrane mixing [37].

For lipids with aliphatic chains, single tailed lipids such as CTAB (cetyltrimethylammonium bromide), have been reported to have low transfection efficiency and high toxicity in plasmid delivery[38]. Although CTAB has proven to efficiently deliver plasmids, it fails to overcome DOTAP in transfection efficiency. Nevertheless, it is possible that for lipids with different headgroups, single acyl-chain lipids may be more efficient [38].

This shows that neither the tail nor the headgroup alone determines the transfection efficiency of a cationic lipid. In an ultimate analysis, one can say that transfection efficiencies depends also on the type of cells that are being used. Therefore, there is not one ideal cationic lipid, but different experiments can be optimized through the use of specific cationic lipids.

1.2.2.Helper Lipids

Besides the cationic lipid, normally a neutral lipid (so-called helper or fusogenic lipid) is included in the lipid mixture[29]. The more commonly used neutral lipids are cholesterol (Chol), 1,2-dioleoyl-*sn*-glycero-3-phosphoethanolamine (DOPE) and 1,2-dioleoyl-*sn*-glycero-3-phosphocholine (DOPC) [30].

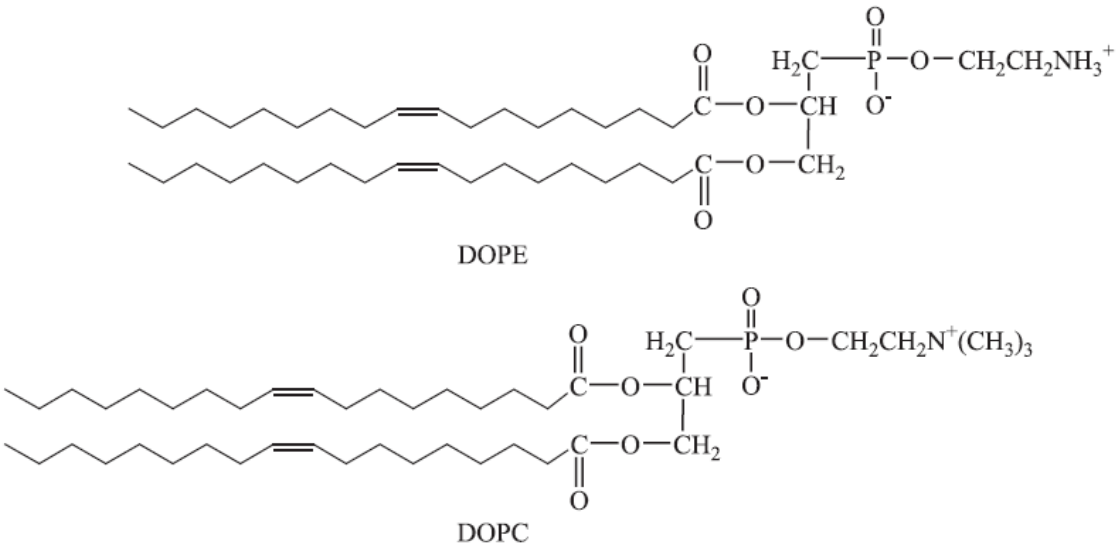

Figure 1.4 Structures of DOPE and DOPC. Both structures are very similar except for the headgroup: DOPE has an ethanolamine group and DOPC has a choline group. This difference is responsible for their different efficiencies has helper lipids. (Figure adapted from Zhang et al 2004)

DOPE has proven to improve transfection efficiencies. It is used in combination with all types of cationic lipids and not only with the ones similar to DOTAP. In vitro studies show that liposomes composed of an equimolar mixture of DOPE and cationic lipids can mediate higher levels of transfection than those containing only the cationic lipid or a different helper lipid, such as DOPC [39,40]. Although DOPE and DOPC share very similar structures, their headgroups are different: DOPE has a smaller ethanolamine group, while DOPC has a choline .[41] The smaller size of ethanolamine gives DOPE a cone shape, increasing its tendency to form the inverted hexagonal phase, especially at acidic pHs, and this may play a major role both in the dissociation of nucleic acids from lipoplexes and on the destabilization of the endosomal membrane [42] as will be discussed ahead. This can be observed in Figure 1.5 (C).

Cholesterol also has been used as a helper lipid. It was shown that DOTAP/Chol complexes are more stable being less affected by NaCl and serum when compared to DOTAP/DOPE complexes. On the other hand,

lipoplex instability is of major importance for an efficient transfection. In this way, in the absence of serum it is preferable to use DOPE, while in presence of serum Chol is preferable, since it grants a higher stability to the DNA:lipid complex, thus increasing the efficiency of gene delivery[43].

Additionally, for in vitro transfection and regarding the formation of the lipoplex, DOPE enables a better matching of charge density of the lipid surface to DNA helices, facilitating counterion release from the lipid surface by DNA and decreasing lipid hydration[43].

1.2.3.From Liposomes to Lipoplexes

Both cationic lipid and helper lipid form a complex with DNA that is capable of efficiently delivering DNA - the lipoplex. This happens because of 3 properties: (1) spontaneous electrostatic interaction between the positively charged headgroup of cationic lipids and the negatively charged phosphate groups of DNA, which results in an efficient condensation of the nucleic acids; (2) an overall net positive charge of the complex lipid-DNA that promotes their association with the negatively charged cell surface and (3) the fusogenic properties exhibited by the cationic liposome formulation that can induce fusion and/or destabilization of the plasma membrane and/or endosomal membrane thus facilitating the intracellular release of complexed DNA[33].

Cationic lipids are capable of spontaneously forming liposomes when placed in an aqueous solution. Liposome size can be controlled according to experiment requirements and the desired properties. There are several methods of preparation of liposomes: hydration of a lipid film, dehydration-rehydration, ethanolic injection, reverse-phase evaporation or detergent dialysis technique [29,44]. Preparation of liposomes through hydration typically requires the following steps: i) solubilization of lipids in organic solvents ii) drying of the organic solvent to a lipid film iii) hydration in aqueous solution[44–47]. A further final step may be performed for the size tailoring of the liposomes, typically a sonication or an extrusion with polycarbonate membranes according to the size required.

When liposomes are put in contact with DNA the positively charged groups of the cationic lipids interact electrostatically with negatively charged phosphate groups from DNA creating a quasi-stable complex. The process has two steps, rapid interaction of anionic DNA with cationic lipids, followed by a slow step of lipid rearrangement[48].

Although liposomes are typically prepared before complexation with DNA, it has been observed that transfection activity is only dependent on the final size of the complexes and not on the size of the liposomes used[49]. It has been shown that regarding complex size, the ratio between the cationic charge of the liposome and the negative charge of the DNA usually controls the size of the lipoplex, whereas preparation conditions such as DNA concentration, pH, buffer composition and salt concentration have less effect. This way, when there is a high positive charge ratio of positively charged cationic lipid to negatively charged DNA, lipoplexes have a size around 200 nm. On the other hand, when a higher content of DNA molecules is present, there is a charge close to neutrality and large aggregates are formed with a size around 1μm[50]. Furthermore at

positively charged cationic lipid to negatively charged DNA charge ratios larger than 1, the DNA is completely protected from the solvent resulting in stable cationic lipoplexes[28].

Regarding the arrangement that cationic lipids and DNA assume within the lipoplex, two types of structures have been observed: a multilamellar structure with monolayers sandwiched between cationic membranes (L^{C}_{α}, Figure 1.5 (A)) and a second one, inverted hexagonal structure sometimes called the inverted "honeycomb" phase, with the DNA encapsulated within cationic lipid monolayer tubes (H^{II}_{C}, Figure 1.5 (B))[29,51]

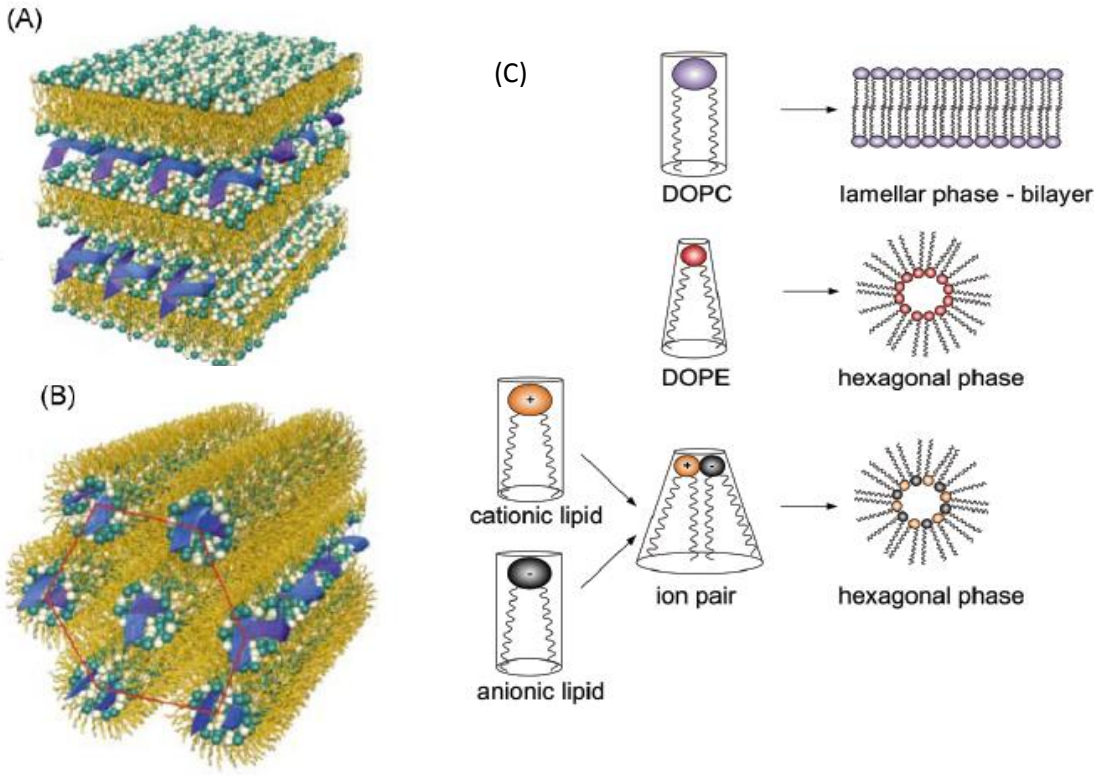

Figure 1.5 Schematic representation of two Lipid-DNA rearrangement within lipoplex structure, the lamellar structure L^{C}_{α} (A) and the inverted hexagonal structure H^{II}_{C} (B). (Adapted from Safinya, 2001) Structures that DOPC and DOPE may assume upon formation of liposomes. Note that even ion pair formation (cationic lipid + anionic lipid) may assume a hexagonal phase, an important step for endosomal escape of DNA (C) (Figure adapted from Nguyen et al, 2012)

Whether lipoplexes assume the first or the second structure is related with the type of cationic lipids used, the presence or not and type of helper lipid and with the lipid/DNA ratio. For example, increasing the concentration of DOPE may promote change from L^{C}_{α} to H^{II}_{C}. This is easily understandable if one recalls the cone-shaped structure of DOPE in opposition to the absence of natural curvature of DOTAP and DOPC, that naturally assume a L^{C}_{α} structure[51]. This observation is depicted in Figure 1.5 (C). Furthermore

complexes assuming a H^{II}_C were directly related to a higher transfection efficiency. This may be due to the fact that H^{II}_C complexes in opposition to the L^C_α are more unstable inside the cells and show fusion of lipids with membranes of the cells and thus eventually promote endosomal escape of DNA[52].

1.2.4.Biological Aspects of Gene Delivery

For an efficient gene delivery to occur, the transgene has to surpass several biological barriers: the plasma membrane, endosomal escape and nucleus entry. Even before reaching the nucleus, the DNA has to avoid being degraded by exonucleases and lipoplexes cannot be dismantled by proteins such as the ones present in serum.

When doing a first approach to this subject it is important to recall that using cationic lipids for the packing of the transgene is already a method to overcome some of the barriers for gene delivery, namely by reducing the surface negative charge, which promotes interactions with cellular membranes. Nevertheless, there are currently still some mechanisms which remain poorly understood or that raise some uncertainties within the scientific community.

The internalization of the lipid-DNA complex is nowadays accepted to be achieved through endocytosis[28,41]. Direct fusion events of lipoplexes with the plasma membrane have been observed but there is no observed correlation of this events with transfection efficiency even with lipoplexes of different charges and constitution[53]. This might be due to the fact that upon lipoplex and plasma membrane fusion, DNA is released into the extracellular space rather than into the cytoplasm[53].

Regarding endocytosis, several pathways are known to be involved in the uptake of non-viral gene delivery systems. Clathrin-mediated endocytosis, caveolae mediated endocytosis, micropinocytosis and phagocytosis are examples of such pathways but the contributions of each one to the internalization of non-viral vectors is not clearly understood[41]. The predominant way of entry seems to be through non-specific adsorptive endocytosis followed by the clathrin-coated pit mechanism[54]. This happens due to the interaction between negatively charged glycoproteins, proteoglycans and glycerophosphates present on the cell membrane and the positively charged lipoplexes[55].

After endocytosis, the normal step is the fusion of the endocytic vesicle with a lysosome followed by degradation. So the release of the DNA from this complex is essential to avoid degradation. This release is the so-called endosomal escape[56].

When using cationic lipids, the so called “flip-flop” mechanism has been suggested to be responsible for the endosomal escape of DNA. Zelphati et al (1999)[57] proposed this mechanism based on the observation of endosomal model vesicles with anionic lipids. It was found that anionic liposomes were able to trigger a rapid release of nucleic acids from lipoplexes. From this observation, it was proposed that once inside the endosomes, there is an electrostatic interaction between the cationic lipids in the lipoplex and the negatively charged lipids from the endosome (mostly found on the cytoplasm facing leaflet). As a result of this

interaction, the endosomal anionic lipids flip-flop across the leaflet and start to laterally diffuse into the lipoplexes, eventually promoting charge neutralized ion pairs with the cationic lipids. This leads to membrane fusion and finally the release of DNA into the cytoplasm[57]. In such mechanism, the presence of DOPE may be decisive for the destabilization of the endosomal membrane[42]. This mechanism is illustrated in Figure 1.6.

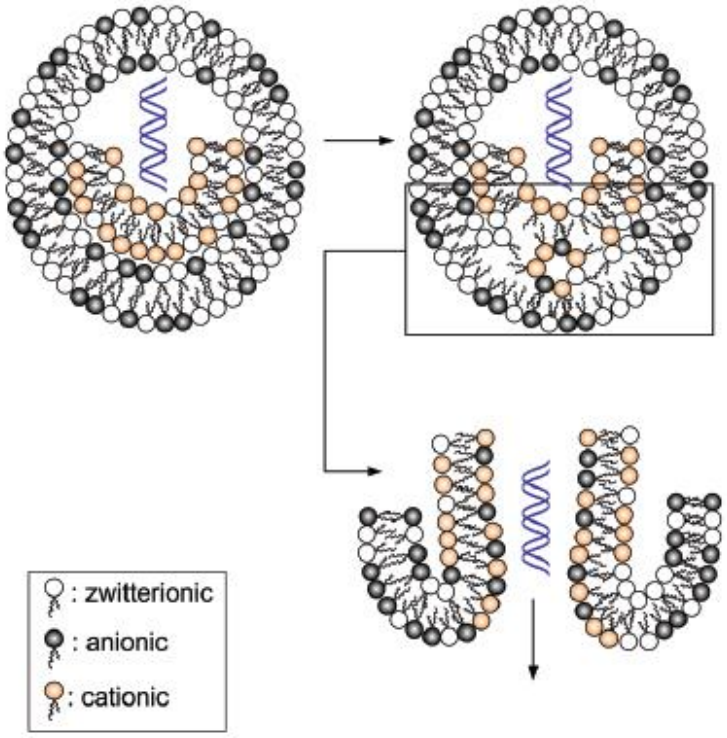

Figure 1.6 Schematic ilustration of the "flip flop" mechanism. Once inside the endosome, cationic lipids and anionic lipids start to establish ion pairs due to electrostatic interaction and charge neutralization. This promotes endosomal and lipoplex membrane fusion and release of DNA into cytoplasm (Image adapted from Nguyen et al, 2012)

Once DNA escapes from the endosome it is released in the cytoplasm and for an efficient delivery to occur it has to reach the nucleus. Microinjection of naked DNA into cells have proven that endonucleases degrade it in a short timescale, thus DNA has to rapidly reach the nucleus to avoid degradation[58].

It is not defined whether DNA comes out of the endosome with some lipids associated or in a naked DNA form. It is important to note that the presence or not of lipids also defines the degree of compaction by which DNA is free in the cytoplasm and reaches the nucleus. But unlike naked DNA, microinjected complexed DNA is not liable of expression[56].

The final barrier for the gene to be expressed is the nuclear envelope and this step is considered to be the major bottleneck in non-viral gene delivery. One of the most accepted routes for DNA import to the nucleus relies on the breakdown of the nuclear envelope, which is a hallmark of mitosis. In this way, any DNA that

is free in the cytoplasm before mitosis M phase is able to enter the nucleus. But this route is only available to dividing cells and thus the transfection of growth-arrested cells, many primary cells and terminally differentiated cells is limited[59].

Other mechanism have been proposed for gene nuclear import, but whether this phenomena relies on active transport mechanisms involving, for example, DNA non-specific association with receptors for nuclear localization signals (NLS) peptides or on passive diffusion mechanisms, remains to be clarified. Entry into the nucleus through passive diffusion is unlikely to occur since nuclear pores exclude macromolecules larger than 70kDa which is significantly lower than the molecular weight of pDNA[33].

Once inside the nucleus, the copy number of DNA and its accessibility for the transcription machinery determines the level of transgene expression. For a measurable transgene expression to occur, a reported minimum of 75 to 4000 plasmid copies have to be delivered to the nucleus, depending on the type of vector[60]. Furthermore, comparisons between different delivery systems showed that higher copy numbers of DNA in the nucleus do not necessarily translates into a higher transfection efficiency.

In conclusion, a deeper knowledge of the mechanisms underlying nuclear delivery of transgenes are certainly needed for a rational optimization of gene delivery methods.

1.3. Current Methods for Reverse Transfection

Traditionally in chemically delivery methods, after the complexation of the DNA with the reagent, the solution with DNA complexes is applied to previously grown cells with a confluence between 70-90% to ensure maximum transfection and minimum toxicity effects. In opposition to the traditional methods, in reverse transfection, the DNA-reagent complexes are first immobilized onto a surface where cells are allowed to grow.

In this section, a review of current reverse transfection methods is carried out before presenting the proposed reverse lipofection technique.

A reverse transfection method is patented. It is a method for high-throughput analysis of gene function in mammalian cells. In this method DNA, cDNA or RNA with known sequences are trapped inside gelatin discs to form spots in a given substrate (Figure 1.7). Then this gelatin is allowed to dry and a lipid transfection reagent is added to the spots. After an incubation period for the interaction between DNA and lipids, the cells are seeded on top of the spots. Following a period of time for transfection and protein expression to occur within the cell, experiments can be carried out [61,62].

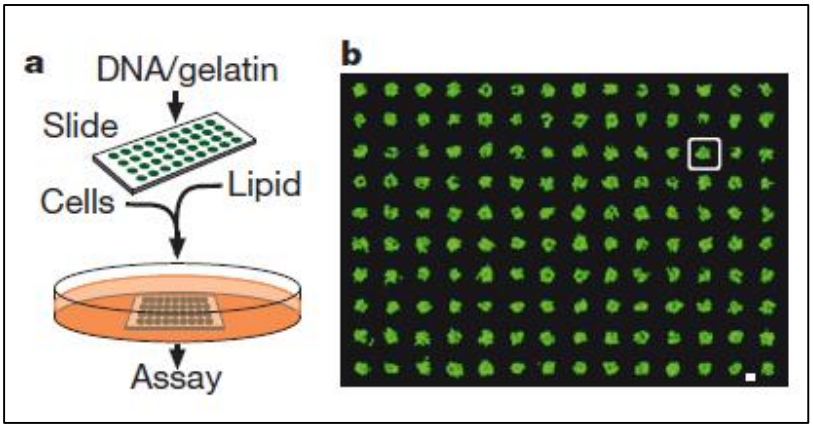

Figure 1.7 Ilustration of the reverse transfection method proposed by Sabatini et al. a) Scheme of the protocol b) cell array expressing GFP reporter gene (Ziauddin et al. 2001)

Several methods of substrate delivery have been described and are mainly applied for tissue engineering with therapeutic purposes. In such systems, the plasmid is trapped inside a polymeric system allowing one of these two cases: a polymeric release where the DNA is released from the polymer, or a substrate-mediated delivery, where the DNA is just retained on top[20]. Examples of these applications include: bone formation by the delivery of a plasmid in collagen in a rat femur[63], induction of a specific IgA by a EVAc (ethylene vinyl acetate) polymer plasmid controlled release in mouse intravaginal mucosa[64] and angiogenesis by injection of a plasmid-gelatin complex in the hind limb muscle of rabbits[65].

The patented method and the polymer delivering method described before represent the two main existing approaches for reverse transfection. In the first, DNA is loaded onto the plates with a polymer (normally gelatin) to promote the long term stability of DNA. Then a carrier and the cells are added sequentially for complex formation[62]. In the second one, DNA and carrier and loaded first with a substrate or onto a substrate and cells are added next[2].

Some improvements have already been purposed for the optimization of these methods. The previous referred works used cell lines easy to cultivate and transfect. Primary cell lines such as human Mesenchymal Stem Cells (hMSC's) were already transfected by the method of spotted DNA[66]. The Retinoblastoma-derived WERI-Rb1 cell line is notoriously difficult to transfect since it is non- or slow dividing, but Reinisalo et al (2005) were able to transfect these cells by reverse transfection efficiently. These authors even reported an efficient freeze drying storage of the polymer/DNA complex until the day of reverse transfection without loss of transfection efficiency[67].

To enhance the uptake of the DNA/reagent complex by regulating the solid-surface conditions, Uchimura et al (2007) proposed a method that uses negatively charged particles of gold colloid (GC) as a nano scaffold for deposition of positively charged Jet-PEI® reagent. These nanoclusters would then be used for DNA condensation and delivery into the cells [68]. DNA can also be co-precipitated with inorganic materials generating DNA/mineral nanocomposite surfaces which can be used for cell culture. The extent of gene

transfer was adjustable by varying the mineral composition. The transfection efficiency was comparable to the one of a commercial lipid and therefore was not optimized[69].

Segura et al (2003) described a method of immobilization of DNA/polymer complexes that allows controlling of the immobilization region and the amount of complex immobilized. PLL and PEI were modified with biotin groups. The resulting complex with DNA is then attached to a neutravidin coated surface[2,70]. Transfection was observed only in the locations where the complex was bound suggesting the possibility of spatially defined DNA delivery[70].

Regarding the immobilization of liposomes, during the development of a method for reverse transfection of non-adherent cells with pDNA deposited on biocompatible anchor for membrane (BAM)-modified glass slides, Kato et al (2003) suggested that the oleyl group in the BAM is targeted for lipid bilayers and so promotes liposomes immobilization [71].

1.4. Aim of the Work and Organization

1.4.1.Aim

The aim of this thesis project is the development and optimization of a novel reverse lipofection technique.

As previously said, traditional methods of DNA chemical deliver, imply that a DNA-reagent complex solution is applied to a 70-90% confluent cell culture previously grown followed by a period of incubation before the cells can be further analyzed. This is the method advised for the use of the commercial reagent Lipofectamine® 2000 from Invitrogen ™ as depicted in Figure 1.8 [72].

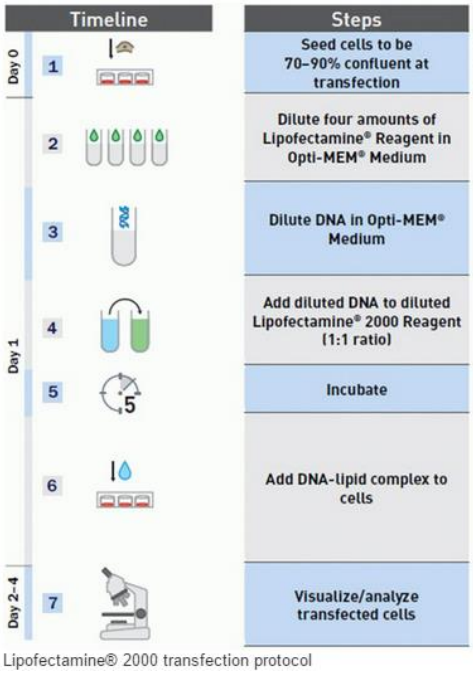

Figure 1.8 Lipofectamine® 2000 protocol as an example for the traditional transfection protocol (http://www.lifetechnologies.com/)

In this work, we propose a new transfection method. Instead of applying the bulk chemical to the cells, the lipoplexes are previously immobilized onto the surface of the culture substrate due to the ligation avidin-biotin: the biotin is incorporated in the lipoplexes as a biotinylated lipid and avidin is attached to the surface of the culture substrate. The binding of avidin to biotin is specific and about four order of magnitude stronger than typical antigen-antibody ligation[73]. Avidin is able to attach to the substrate and therefore is able to immobilize biotin ligated compounds. Avidin coated surfaces for the immobilization of several biomolecules containing biotin is a well-established tool with different areas of application[74].

Cells are then seeded on top of the lipoplexes and allowed to grow. The current research for efficient transfection methods is mainly focused on methods to be applied for therapeutic purposes. On other hand this proposed method is likely to allow the combination of cell array technologies with a simple transfection methodology. Furthermore, the use of immobilized lipoplexes may improve the existing reverse transfection methods in terms of ease and readiness for use. A schematic representation of this proposed lipofection technique is depicted in Figure 1.9.

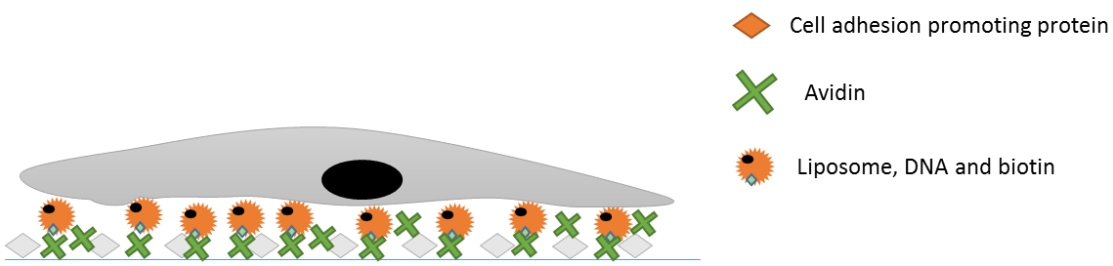

Figure 1.9 Schematic representation of the proposed reverse lipofection technique. Cells are seeded on top of immobilized lipoplexes due to avidin-biotin ligation. A cell adhesion promoting protein is also used.

Since in general the biological aspects of gene delivery methodologies are poorly understood, when dealing with a new technique, one tries to understand some of the biological features underlying the transfection. In this sense, during the development and optimization of this method, we also aimed to characterize some of these biological features.

1.4.2.Novelty and Advantages

In this new proposed method several characteristics are already established components of gene delivery as previously stated throughout this work. (1) Cationic lipids and liposomes are widely used as a standard technique, either for gene delivery or for other purposes. (2) Reverse transfection as a methodology where DNA/carrier is applied first before cell seeding is also a common technique. (3) As seen before, some DNA/carrier immobilization techniques have also already been applied. (4) Furthermore, immobilization of liposomes by biotin-avidin ligation or other systems has also been used for many different goals.

Although immobilization of vesicles taking advantage of the affinity between biotin and avidin/neutravidin is not a new approach, it is a novelty when applied to immobilize lipoplexes for reverse gene delivery to cells. This way, one can combine the advantages of lipid-assisted transfection with the advantages of lipoplex immobilization. This immobilization is likely to allow for spatially defined DNA delivery, for example in a patterned surface. In this way, high-throughput analyses of multiple genes can be performed using the same surface and thus reducing the error and variation between samples. On the other hand, even when the same surface is not required and the analysis have to be carried out in well-plates, the uniform coating of avidin and specificity of ligation with biotinylated lipids in the lipoplexes, is expected to allow for more uniform transfection conditions from well to well, thus reducing the error.

One advantage of reverse transfection with cationic lipids is that it may have a reduced toxicity when compared to the traditional method and the need for a high confluence is abolished. Furthermore, the concentration of cationic lipids applied is lower and since cells are seeded on top of lipoplexes there might be a continuous release of the DNA into the cells. Also, since cells are all seeded in a single event, they are subjected to the DNA at the same time and likely at the same cell cycle phase. Otherwise, in traditional

bolus delivery, cells are seeded and allowed to grown for a given time before exposure to transfection agents, and so cells going through different cell cycle phases coexist in the same sample.

1.4.3.Organization

This work has been divided into two main parts.

The first part consisted of a proof of concept of the method regarding both the immobilization of lipoplexes and the transfection of HEK cells. In this sense, different immobilization of liposomes/lipoplexes were tested and from what seemed to be the most stable condition, transfection of cells with such system were tested. Regarding the transfection, several parameters were tested. In this first exploratory part of the work confocal and multiphoton microscopy was used. This way it was possible to have a better insight of the behavior of both lipoplexes and cells upon experimental conditions.

Secondly, by means of experimental design using Response Surface Methodologies (RSM), the optimization of the reverse lipofection methodology was performed. Since in the first part it was possible to perceive the influence of several variables in the transfection efficiency, the influence of these variables was analyzed in greater detail in this second part of the work. The relationship between these variables was also assessed. Five variables were considered: lipid concentration, DOTAP:DOPE proportion, initial number of cells, pDNA concentration and liposome size. At this stage of the work a faster and high throughput analysis of the cells was required and therefore flow cytometry was performed.

In the following sections, an analysis of the advantages of the use of confocal/multiphoton microscopy and flow cytometry in the context of this work is explored. Furthermore, the same contextualization is done for RSM.

1.4.4.Complementing Flow Cytometry with Confocal/Multiphoton Microscopy in the Context of the Work

Over the past years fluorescence microscopy, fluorescence labeling and imaging methods were the aim of exhaustive investigation for an increased detection sensitivity and ultra-high spatial-temporal resolution. As a consequence of this development, these techniques play now a crucial role in the characterization of cellular and subcellular structures as well as providing insights on cellular pathways, functions and specific interactions taking place at the cellular level[75–77].

Confocal microscopy basic concept is the use of spatial filtering techniques that eliminates out-of-focus light due to the use of a pinhole. This allows to control the depth of field and more important in biological applications it allows the collection of serial optical sections from thick specimens [78].

Multiphoton microscopy was also used in this work. In standard fluorescence microscopy, single photon excitation is used to excite fluorophores from a ground state to an excited state (Figure 1.10). When returning to the ground state from an upper energy level, energy is released in the form of a photon which

can be detected with a photomultiplier or another detection system. In multiphoton excitation, typically two photons are used to excite the fluorophores. Therefore an excitation light with about twice or more the wavelength of single photon absorption peak is used [79]. Typically, a multiphoton microscope uses a pulsed infrared laser (usually a Titanium: Saphire (Ti:Sa) laser) with a tunable range between 700 and 1000nm.

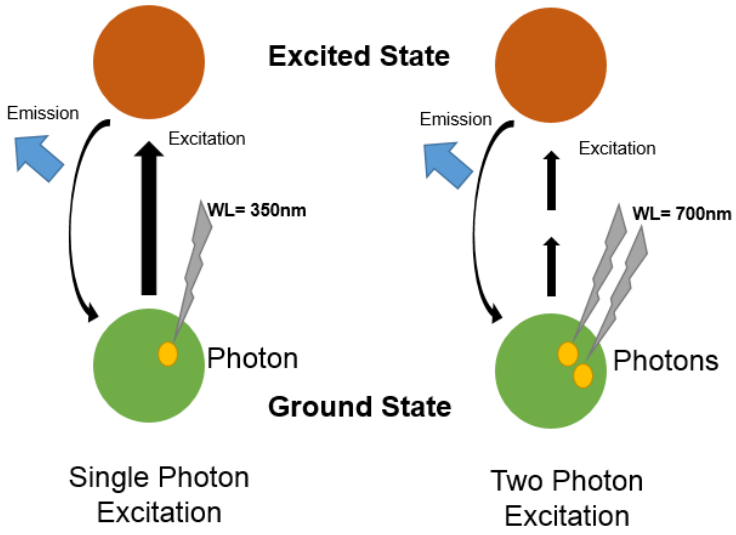

Figure 1.10 Scheme illustration of the difference between single photon excitation (confocal microscopy) and two photon excitation (multiphoton microscopy)
(Figure adapted from http://www.olympusmicro.com/primer/techniques/confocal/applications/multiphoton.html)

Multiphoton excitation occurs only in a very restricted spatial focus, since it requires very significant radiation power, which is only observed in a small volume along the laser excitation profile. Therefore the use of pinhole in multiphoton is no longer needed since the excited fluorophores are found in a volume comparable to the confocal volume. This means that confocal and multiphoton microscopy have comparable resolutions, but the theoretical principles behind each are very different[79].

The main advantage of the use of multiphoton microscopy is its ability of very long wavelength light to penetrate deeper in the tissues, allowing visualization of thick samples. It also has the advantage of reduced photodamage and the lack of out-of-focus bleaching. However, the use of multiphoton microscopy in the context of this work is only associated to the inability of exciting commonly used nucleus probes with the available single photon excitation lasers in the confocal microscopy.

The main advantage when using either confocal or multiphoton imaging methods , is that one is able to visualize living cells without any preparation protocol like staining (as in histochemistry techniques) or fixation (like in flow cytometry). On the other hand, no further work is needed (like for example in PCR

methods) since a simple image is took at the time of the visualization. In this way, artifacts associated with cellular manipulation are avoided.

However, these two techniques lack the possibility of processing a large amount of data, as the measurement of the percentage of transfected cells is limited to the measured area per each image. But most importantly, even though one may take several images to acquire data on a maximum number of cells, only a very small portion of the population is being observed. In this way, an accurate analysis of the cells upon experimental conditions may be impaired. In opposition, flow cytometry allows for the analysis of the whole population and hence is likely to recover more robust results. Furthermore it is fast, simple and the most used technique to analyze populations of cells for different purposes.

1.4.5.Response Surface Methodologies

RSM consists of a set of statistical methods that can be used to improve and optimize bioprocesses. It is typically used in situations where several factors influence one or more desired response variables, in this case the transfection efficiency[80]. It is used for the optimization of many different types of bioprocesses [80–82].

Traditionally, optimization procedures comprise several assays to determine which condition is better for a maximum response variable and typically only one variable is changed at a time. This implies that the effect that different variable may have on each other is not considered, as to do so, would require carrying out a massive number of experiments if a great number of variables and a large experimental region of values is under scrutiny RSM is used to overcome these issues as the most used multivariate statistics technique.

RSM is a collection of mathematical and statistical techniques based on the fit of a polynomial equation to the experimental data, which must describe the behavior of a data set with the objective of making statistical previsions. But before applying the technique it is necessary to define which should be the experimental design that will define the set of experiments to be carried out within the experimental region under study.[83] For RSM it is necessary to have a quadratic model so it is necessary to use designs such as the Box-Wilson Central Composite Design (CCD)[84].

CCD allows the generation of a second order (quadratic) model for the response variables without the need of a complete three level[80]. This design consists of the following parts: (1) a full factorial or fractional design; (2) an additional design, often a star design in which experimental points are at a distance α from its center and (3) a central points[83]. Within the CCD in this work it was used a Face Centered Design (CCF). In this design, the star points are at the center of each face of the factorial space and thus $\pm\alpha=\pm1$. In this way, there will be three levels (-1, 0, +1) for each factor. If the design in use is not face centered 5 levels of each factor would be required[83,85].

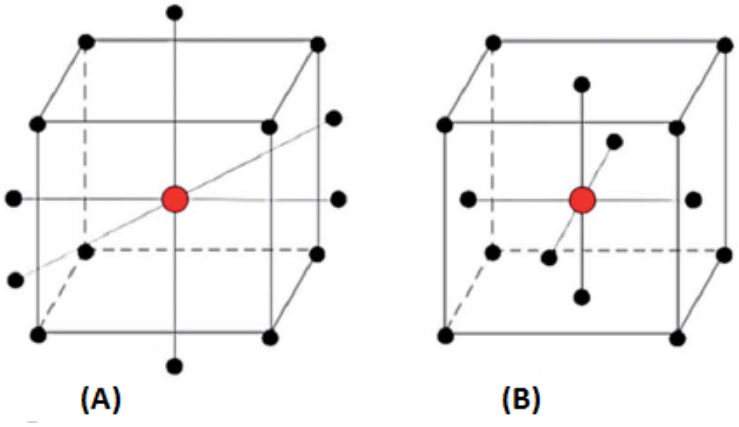

Figure 1.11 Schematic representation of the differences between central composite design CCD (A) and face centered central composite design CCF (B). Notice that in CCF star points are ate the face of the factorial space (Adapted from Lebed et al, 2013 [86])

Once the design is executed and the results are obtained, one can apply RSM technique. Notice that the design is the first step followed by: (2) modelling, (3) validation and (4) optimization. In the second step, modelling, the response variable(s) is/are expressed as a function of the independent variables. Then this model is evaluated by means of statistic validation. Finally, the response surface plots are drawn and from this, conclusions can be taken.

2. MATERIALS AND METHODS

2.1. Plasmid DNA Production and Purification

The plasmid DNA used was pVAX1GFP (3697bp), which is based on the commercial available pVAX1LacZ (6050bp) from Invitrogen, where the LacZ gene was replaced by GFP gene[87]. For replication inside bacteria, the plasmid has a pUC origin and a Kanamycin resistance gene to maintain selective pressure.

The vector also contains the human cytomegalovirus immediate early promoter (CMV promoter) that allows GFP expression in mammalian cells. The plasmid also includes a bovine growth hormone polyadenylation sequence (BGH PolyA)[88]. Since GFP is expressed upon efficient expression it was chosen as the reporter protein for these transfections assays.

Plasmid DNA was replicated in strain DH5α of *E.coli*. First a pre-inoculum was prepared in 5 mL of Luria Bertani medium (LB) (NZYTech) overnight. Then an inoculum culture was started at an Optical Density (OD) of 0.1 in 50 mL of LB. This inoculum was grown until an OD=1 and then used to inoculate 500 mL of LB for the final culture, starting with an OD=0.1. Finally, this final culture was grown overnight and reached a final OD of 4. Media pH was adjusted to 7.5 before autoclaving. All media were supplemented with 1% (v/v) of Kanamycin to maintain selective pressure and growth was performed at 37ºC and 2500 RPM.

When growth was over, the culture was centrifuged at 6000 G's for 15 minutes at 4ºC. Supernatant was discarded and pellet was kept at -20ºC until further use.

For plasmid purification, the QIAGEN® HiSpeed Plasmid Maxi Kit was used according with manufacturer instructions. This kit comprises 6 main steps, starting with an alkaline lysate of the bacteria, followed by a clearing of the lysate by filtration and binding/elution of the plasmid DNA to/from a resin of a HiSpeed tip (included in the kit). The final steps include precipitation with isopropanol (0.7 volumes) and a specific precipitator included with the aim of getting ultrapure plasmid DNA.

Additionally, in one experiment, the same plasmid purified by two other methods were used. This two methods included a MiniPrep Kit (High Pure Plasmid Isolation Kit, Roche) and a Hydrophobic Size Exclusion Chromatography (Hic-Sec) as described by Diogo et al [89].

Plasmid DNA final concentrations were obtained using Nanovue Plus Spectrophotometer (GE Healthcare). In order to assess plasmid quality and dominant isoforms, a 1% agarose gel with TAE buffer (40mM Tris-acetate and 1mM EDTA) was run at 100 mV for 1h. The gel was post stained in ethidium bromide solution (0.5µg/ml) and then observed, integrated and photographed with an ultraviolet transillumination equipment (Eagle Eye II, version 1.1, Stratagene) with a camera system. Ethidium bromide intercalates into DNA strands and allows for DNA detection under UV light.

2.2. **Human Embryonic Kidney (HEK) Cell Culture**

2.2.1.Culture Medium and Other Reagents

In this work, the cell line used was Human Embryonic Kidney 293T (HEK 293T). HEK 293T cell line is a derivative cell line from HEK 293. The difference consists in the presence of SV40 T-antigen, which increases transfection efficiency in HEK 293T cells. It is widely used for retroviral production, gene expression, and protein production. (http://www.lgcstandards-atcc.org/) Herein it will be further referred as HEK.

Medium used for HEK cell culture was Dulbecco's Modified Eagle Medium (DMEM) (Gibco ©) supplemented with 10% Fetal Bovine Serum (FBS) heat inactivated (Gibco © Lot 1176955) and 1% PenStrep (Gibco ©) containing 10000 Units/mL of Penicilin and 10000 µg/mL Streptomycin. For the preparation of the medium all components were filtered together in a RapidFlow™ Sterile Disposable Filter Units (0.22µm pore Polyethersulfone (PES) membrane, Nalgene™) inside a flow chamber.

When mentioned, Poly-L-Lysine (PLL) was used to promote cell adherence onto the solid substrate. For this, a 10% (v/v) of PLL 0,1% (Sigma ®) was applied onto the substrate before cell seeding or experience assemble.

For cell and substrate washing and dilutions a Phosphate Buffer Solution (PBS) 1x pH 7.4 (Gibco ©) was used. For the preparation of the 10x final solution, 100 mL of PBS 1x was diluted in 900mL of milipore water and then autoclaved for 20 minutes at 121ºC.

For cell fixation, a 2% PFA (Paraformaldehyde) was used. A 4% PFA solution was paper filtered, aliquoted and stored at -20ºC. At time of use, aliquots were thawed at 37ºC until they became clear (after thawing there is precipitate formation) and diluted with PBS to 2% final concentration.

2.2.2.*Freeze, Thawing and Culture Conditions*

When not in use, aliquots of $3x10^6$ cells were preserved at -80ºC in the culture medium and supplemented with 10% Dimethyl Sulphoxide (DMSO) (Sigma®)

For thawing, a vial of frozen cells was allowed to thaw until only a few crystals of ice/DMSO were present and then diluted into 5 mL of culture medium. Then it was centrifuged at 1500 rpm for 5 minutes and supernatant completely discarded to ensure absence of DMSO. Finally the cell pellet was resuspended in 1mL of culture medium.

Cells were then plated in T-flasks of $25cm^2$ with vented caps (Falcon BD) in 5 mL culture medium and allowed to grow (37º, 5% CO_2, humidified environment) until 70-80% confluence. When this confluence was reached, cells were replated. For this, exhausted medium was first collected and cells washed with PBS

followed by detachment of the cells by adding 2ml of TrypLE reagent (Protease, EDTA and Inorganic Salts, Gibco©) and incubation at 37º for 5 minutes. Then, 3mL of complete medium were added and the suspension centrifuged for 5 minutes at 1500 rpm for cell pelleting. After this, the cell pellet was resuspended in 1mL of complete medium and cells were plated at 4000 cells/cm^2 into a new flask with flesh medium.

2.2.3.*Cell Nucleus Probing*

In imaging experiments, cells were counted through nucleus staining with Hoescht 3342 (Fischer Scientific). 2µM aliquots of Hoescht 3342 were prepared in PBS and stored at -20ºC until used. For imaging experiments, 200uL of this solution was applied to the wells and incubated for 10-15 minutes at 37ºC. Since this probe is very specific for the nucleus and displays a very low background staining, a single PBS wash was performed and cells were ready for visualization.

2.3. **Preparation of Lipid Vesicles**

2.3.1.*Lipids*

The liposomes used in this work were prepared using the cationic lipid 1,2-dioleoyl-3-trimethyl-ammonium-propane (DOTAP) and the zwitterionic lipid 1,2-dioleoyl-*sn*-glycero-3- phosphoethanolamine (DOPE). A biotinylated lipid 1,2-dioleoyl-*sn*-glycero-3-phosphoethanolamine-N-(cap biotinyl) (DOPE-Cap-biotin) was also used in all liposome formulations to promote the immobilization of the lipoplexes onto the substrate (via ligation with avidin).Biotinylated lipid incorporated in lipid mixtures at a ratio of 1 biotin molecule to 1x10^6 lipid molecules (1: 1x10^6)

When labeling of the liposomes or lipoplexes with fluorescent dye was required, 1,2-Dioleoyl-sn-glycero-3-phosphoethanolamine-N-(lissamine rhodamine B sulfonyl) (DOPE-Rho) was used. This molecule was incorporated at lipid mixtures at a ratio of 1 DOPE-Rho molecule for 200 lipid molecules (1:200).

DOTAP and DOPE have similar molecular weights, 698.55 and 744.04g/mol, respectively. In this way all lipid formulations (DOTAP:DOPE proportion) herein described were assumed to have the same molecular weight. All lipids were from AVANTI® Polar Lipids.

2.3.2.*Lipid Vesicles Preparation*

Three different formulations were used in this work regarding DOTAP:DOPE proportions, 1:1, 1:3 and 3:1, and all of them were prepared in chloroform for a final concentration of 1mM after PBS hydration.

To this end, the desired amount of lipid was first measured from lipid stock with glass syringes. Since chloroform is toxic and cannot be present in cell culture, lipid formulations were then dried under N_2 stream and left in vacuum overnight to ensure chloroform exhaustion. This results in a thin layer of lipids in a film that was kept at -20ºC until further use.

For preparation of liposomes, the lipid film was suspended in PBS to the final lipid concentration of 1mM. Three cycles of heat (60ºC) and vortex and five freeze-thaw (60ºC- liquid N_2) cycles were performed to homogenize the lipid mixture. Since lipids are amphiphilic (hydrophobic tail and hydrophilic head) molecules, vesicles spontaneously formed when placed in an aqueous solution such as PBS.

Finally, the lipid vesicles were tailored according to the experiment. To obtain Small Unilamellar Vesicles (SUV's) (+/- 50nm), sonication was performed at room temperature for two minutes. To obtain Large Unilamellar Vesicles (LUV´s), an extruder, LiposoFast Basic (Avestin) was used with 100 nm and 400 nm-pore-size polycarbonate membranes. During extrusion, the lipid mixture is forced to pass through a pore of determined size which homogenizes the liposome dimensions to the one of the pore. The lipid solution was extruded 21 times.

2.4. Reverse Lipofection Setup Assemble

The reverse lipofection technique proposed in this work comprises three main steps: surface coating, lipoplex preparation and immobilization and cell seeding. For the preliminary assays, 8-well IBIDI microscopy chambers were used. For the optimization assays using RSM, 24-well plates were used since the analysis of the cells were performed by flow cytometry and a greater number of cells was necessary for this purpose.

The first step was the coating to promote cell adherence to substrate. For this, PLL was used as previously stated. PLL was allowed to adhere for 1h. After, the wells were washed 3 times with PBS to remove any traces of PLL that did not adhere. Avidin (from egg white, Sigma ®) 0,1mg/mL solution (in PBS) was applied in each well and allowed to adhere for 3h. After, the same washing step was performed. Both incubations were carried out at room temperature inside a flow chamber.

It should be noted that neither concentrations of biotinylated lipid nor avidin were optimized in this work. As previously referred, liposome immobilization has already been used for different goals and these quantities were already optimized.

For preparation of lipoplexes, three different lipid concentrations (in PBS) were used: 3.6, 7.2 and 14.4 ng/µL. 5 minutes after dilution of the lipid vesicles to the desired concentration, 0.5, 1, 2 or 4 µg of plasmid DNA were added to 500 µL of lipid solution. This results in pDNA final concentrations of 1, 2, 4 and 8ng/µL. Since DNA has to interact electrostatically with the cationic lipid a 20 minute incubation time was used. Only after this period, lipoplexes were added to the wells for immobilization. This was also performed at room temperature inside the flow chamber for 1h.

During the one hour allowed for lipoplexes immobilization, cells were prepared for plating. For this, cells were detached from the T-flask according to the protocol described before. Cells were counted by the Trypan Blue exclusion method under an inverted protocol. When assays were performed at 8-well IBIDI microscopy chambers, cells were plated at 30000 cells/cm^2. For the RSM assays in 24-well plates, different

initial number of cells were used: 17000, 25000 and 34000 cell/cm^2. Cells were then allowed to grow for 72h at 37ºC in humidified environment with 5% CO2. Also, for this assays, only cells between passages 5 and 10 were used. Before cell seeding wells were washed with PBS to remove non-adherent lipoplexes.

The following table summarizes the volumes used of each reagent and solution. The volumes were used according to the growth area of the wells, 1cm^2 and 2cm^2 for IBIDI chambers and 24-well plate, respectively.

Table 2.1 Summary of the volumes used for Medium, TrypLE, PBS, avidin and lipid solution in IBIDI chambers and 24-well plate for the reverse transfection assays (confocal/multiphoton microscopy and cytometry, respectively)

Reagent/Solution	**Type**	
	IBIDI Chambers (µL)	24-well plates (µL)
Culture Medium	200	400
TrypLE	80	200
PBS for well washing	200	400
PBS for cell washing	400	800
Avidin Solution	200	400
PLL solution	200	400
Lipid Solution	200	400

2.4.1.*Liposomes/Lipoplexes Immobilization Assays*

In these assays, both immobilization of liposomes and lipoplexes were used, which means that only on the second case pDNA was added to the lipids solution. These assays were performed in 8-well IBIDI chambers and no cells were used. Lipid vesicles conditions were: DOTAP: DOPE proportion 3:1; total lipid concentration of 14.4ng/µL and 2ng/µL of pDNA for lipoplexes formation. Also, for the detection of the vesicles through confocal fluorescence, all lipid mixtures contained the lipid fused with Rhodamine (DOPE-Rho).

IBIDI chambers wells were coated according to the experience design. For this, 4 different coatings were used: no coating (chamber substrate); avidin coating (0.1 mg/mL); PLL coating; and both avidin and PLL coating. All coatings were performed the same way as for cell assays.

In these assays only SUV's were used and their preparation was made accordingly to what was described in the previous sections. After dilution and 5 minute incubation liposomes were immediately immobilized. Lipoplexes were immobilized after the addition of pDNA to the liposomes and a 20 minute incubation. In both situations, before confocal microscopy visualization, an incubation period of 1 h was performed and 3 steps of PBS washing were carried out to remove all non-immobilized liposomes/lipoplexes.

2.4.2.Charge Ratios Calculations

For an accurate comparison of the results with bibliography, the charge ratios (+/-) of the lipoplexes used was calculated.

Charge ratios (+/-) is defined as the number of amines on the cationic lipid relative to the number of phosphate groups[90]. For this, it was established a relation of 3 nmol of phosphate per µg of DNA[91]. DOTAP molecules have a single amine.

Table 2.2 Calculation of lipoplex charge ratios. On the left: Concentration of amine present for each DOTAP:DOPE proportion at different concentrations. On the right: Concentration of phosphate per amount of DNA. In blue: charge ratios for all the lipoplexes compositions used in this work

			pDNA (amount (µg) and nmol of phosphate)			
	DOTAP:DOPE proportion	**[amine] nmol**	0.5 µg	1 µg	2 µg	4 µg
			1.5	3	6	12
18 µg	1:1	1.25	0.83	0.42	0.21	0.10
	1:3	0.58	0.39	0.19	0.10	0.05
	3:1	1.87	1.25	0.62	0.31	0.16
36 µg	1:1	2.5	1.67	0.83	0.42	0.21
	1:3	1.16	0.77	0.39	0.19	0.10
	3:1	3.74	2.49	1.25	0.62	0.31
72 µg	1:1	5	3.33	1.67	0.83	0.42
	1:3	2.32	1.55	0.77	0.39	0.19
	3:1	7.48	4.99	2.49	1.25	0.62

2.5. **Confocal and Multiphoton Microscopy**

Fluorescence imaging was carried out on a Leica TCS SP5 inverted confocal laser scanning microscope (Leica Microsystems CMS Gmbh). The excitation lines provided by the argon laser were focused into the sample by an apochromatic water immersion objective (63x, NA 1.2; Zeiss Jena Germany). The out-of-focus signals were blocked by using a 111.4 µm-diameter pinhole in front of the image plane. The emission was detected through the spectrophotometric detection system of this microscope.

Three different fluorophores were detected by confocal microscopy: GFP (when an efficient transfection occurred), Rho-DOPE (liposomes) and Hoechst 33342 (nucleus). GFP imaging was achieved through excitation with an Ar 476 nm laser and detection at 500-560 nm. Rho-DOPE fluorescence data acquisition was carried out with excitation with an Ar 514 nm laser and detection at 550-650 nm.

Multiphoton excitation for imaging of Hoechst 33342 was carried out in the same Leica TCS SP5 inverted microscope but with a Titanium-Sapphire (Ti:Sa) laser as the excitation light source. The excitation wavelength was set to 780 nm and the fluorescence emission was collected at 400-460 nm.

2.5.1.*Microscopy Image Treatment*

Merging of the images with Hoechst 33342 and GFP and counting of the cells was achieved with ImageJ Software.

Transfection efficiencies were calculated by counting the number of transfected cells (which showed GFP fluorescence) and dividing it by the total cell number. For each sample 3-5 random images were acquired within different areas of the well.

2.5.2.*Flow Cytometry Assay*

After 72 h of reverse transfection, cells were washed carefully with PBS to avoid detachment and then pelleted as described before. After centrifugation, the supernatant was discarded and cell pellet was resuspended in 600 µL PBS supplemented with 2% PFA and kept at 4ºC until analysis.

The equipment used was a FACScan Scalibur (Becton-Dickinson) that recorded the forward scatter (FSC), side scatter (SSC) and green fluorescence (FL1) in each run. Therefore, for each sample, cells were isolated from the debris due to their characteristics of FSC versus SSC, which defined a gate that distinguished cells from debris that were outside the gate. Background autofluorescence of non-transfected cells was taken into account to determine transfection efficiencies, considering the difference between total cell population inside the gate, and the background autofluorescence of non-transfected cells, indicated by FL1 parameter [87]. This established the M1 and M2 parameters, corresponding to non-transfected and transfected cells with green fluorescence, respectively.

Data was analyzed and green fluorescence intensity corresponding to GFP expression level, histograms and dot plots were generated with CellQuest Pro Software © (Becton Dickinson).

2.5.3.Data Treatment

Four independent replicates of each 30 set of assays were obtained. For a flow cytometry assay to be statistically significant, a minimum of 1000 events must be measured. Therefore, assays with less than 1000 events were not considered. For this reason, for some conditions only 2-3 (out of 4) replicates were used.

Statistical analysis of flow-cytometry data was carried out after normalization of transfection efficiencies of each 30 assays to the maximum transfection efficiency obtained within 30 assays set. This accounted for some variation observed in assays performed in different days. After this, mean values and standard deviations for replicates were calculated and introduced in RSM.

Absolute values obtained for transfection can be consulted in the Annex.

2.6. Surface Response Methodologies for Process Optimization

Aiming at the optimization of the reverse transfection technique, the effect of total lipid concentration, DOTAP:DOPE proportion, cell initial number, pDNA concentration and liposome size in transfection efficiency was assessed using a Central Composite Face Centered (CCF) design with the assistance of STATISTICA software (StatSoft). Furthermore, it was also possible to assess relations between these variables and the effects that each one has on the others.

For the design setup, three different coded levels for each variable were used- low (-1), center (0) and high (+1) (Table 2.3) according to what was obtained in preliminary assays, with four repetitions at central point. The response variable was the percentage of transfection measured as the fraction of cells efficiently transfected (expressing GFP) within the entire population of cells measured by flow cytometry.

Table 2.3 Coded and uncoded values for the five factors and levels

Factors	Description	Levels		
		Low (-1)	Center (0)	High (+1)
X_1	Lipid concentration (ng/µL)	3.7	7.2	14.4
X_2	DOTAP:DOPE proportion	0.33	1	3
X_3	Initial cell number (cells/cm^2)	17000	25000	34000
X_4	pDNA concentration (ng/µL)	1	4	8
X_5	Liposome size (nm)	50	100	400

A CCF design allows the estimation of a full quadratic model with the following general description: number of experiments $(n) = 2^{k-p} + 2k + cp$ where k is the factor (variable) number, p is the fractionalization number and cp is the center points required for curvature estimation which gives a planned design of 30 experiments ($30 = 2^{5-1} + 10 + 4$) listed in Table 3.2.

2.6.1. *Model Building, Fitting and Evaluation*

A quadratic model that included linear and quadratic main effects plus two-way interactions was fitted to the data as follows:

$$\%\,Transfection = b_0 + b_1X_1 + b_2X_2 + b_3X_3 + b_4X_4 + b_5X_5 + b_1X_1^2 + b_2X_2^2 + b_3X_3^2 + b_4X_4^2 + b_5X_5^2 + b_{12}X_1X_2 + b_{13}X_1X_3 + b_{14}X_1X_4 + b_{15}X_1X_5 + b_{23}X_2X_3 + b_{24}X_2X_4 + b_{25}X_2X_5 + b_{34}X_3X_4 + b_{35}X_3X_5 + b_{45}X_4X_5$$

The statistical significance of the full quadratic model predicted was evaluated by the analysis of variance (ANOVA) and least squares technique. Also the significance and the magnitude of the effects estimates on

each variable were determined. ANOVA is a flexible data analytical technique that allows us to test hypothesis, typically about population means. In the particular case of surface response analysis, the null hypothesis (H0) is that the predictive model does not fit the experimental data significantly better that an horizontal line equal to the mean, using a Fisher's F-distribution as part of the test of statistical significance. This way all the factors were tested to determine which ones had an effect statistically significant for in the response variable. Effects with less than 95% of significance, that is, effects with a p value higher than 0.05, were discarded and pooled into the error term (residual error) and a new ANOVA was performed for the reduced model.

The experimental data was replicated at the central point. This means that these points were taken under identical experimental conditions. In this way, it is possible to estimate the error variability (commonly referred to as the pure error) of the experiment from the variability of the replicated runs and hence still divide the residual variation into two portions: one that accounts for the unreliability of the response variables measurements (random or pure error) and other that accounts for all remaining variability that cannot be explained by the factors and respective interactions present in the model neither by lack of fit.

The significance of the model can be evaluated by considering either the F-values or the p-values of the model and the lack of fit. The F-values are determined by the ratio of the mean square (MS) of the parameter in study to the MS of the error term, while the p-values can be computed from the F distribution (given the F-value and the degrees of freedom of the parameter in study and the error term). In the case of the lack of fit, the F-value is determined using the MS of the pure error instead of the residual error.

MS represents the average square deviations around the grand mean. It is calculated by dividing sum of squares (SS) by the corresponding degrees of freedom.

A final step of ANOVA was to perform a LOF test to compare the residual error and the pure error from replication. This is achieved by estimation of the LOF F-value statistic (by the ratio of the mean square of the LOF to the mean square of the pure error) and the corresponding probability (p-value). If, in fact, the residual variability is significantly larger than the pure error variability, then one can conclude that there is still some statistically significant variability left, and hence, there is an overall lack of fit of the current model and another model may be more appropriate.

The regression model was accepted when the p-value of the model was lower than 0.05 and the lack of fit higher than 0.05. However, if any of these conditions was not fulfilled, the model was only accepted when the model correlation coefficient (R^2) was higher than 0.70 which means that 70% of the data was explained by the model.

3. RESULTS AND DISCUSSION

3.1. Plasmid DNA Assessment

The quality and purity of plasmid pVAX1GFP was assessed by agarose gel electrophoresis. The result is present in Figure 3.1.

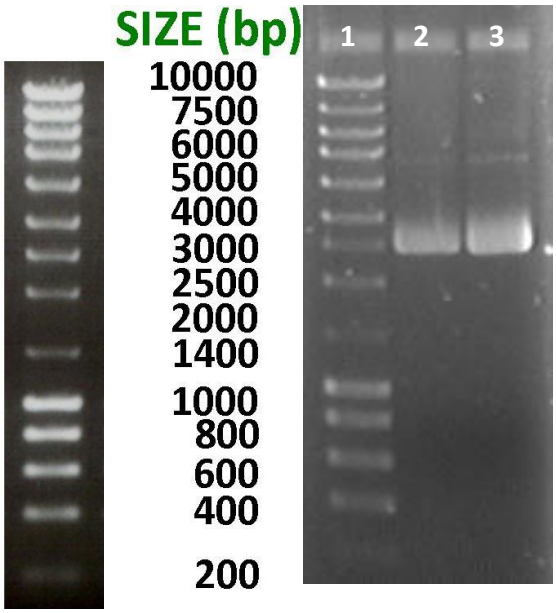

Figure 3.1 Electrophoresis gel of the purified plasmid. First lane is for the molecular ladder (NZYDNALadder II, NZYTech) while the second and the third are for 300 and 500 ng of plasmid DNA

Lanes 2 and 3 show 300 and 500 ng of pDNA, respectively. The majority of the plasmid is presented in a band between the 2500 and 3000 bp corresponding to the super coiled isoform. In this way, the plasmid was in the appropriate conditions to be used in transfection assays.

3.2. Immobilization of Liposomes and Lipoplexes

The novelty of this work is the immobilization of lipoplexes. Many authors have already described the immobilization of liposomes using the ligation of avidin-biotin[92,93] but this system has not been applied to the immobilization of lipoplexes for reverse transfection. In this sense it was necessary to test the immobilization of lipoplexes (in comparison to liposomes) in cell culture condition. Therefore immobilization efficiency was tested in the presence of cell culture medium (complete DMEM) and of cell adhesion promotion coating, which in this work was based on Poly-L-Lysine (PLL)

In this way, the following conditions were tested: no coating (glass), PLL coating, avidin coating and PLL+avidin coating. Also, both lipoplexes and liposomes alone were tested. At this exploratory stage of the work, some conditions were established: 2ng/µL of pDNA and for the liposomes a total concentration of 14.4ng/µL at DOTAP: DOPE proportion of 3:1. SUV's prepared by sonication were used in all formulations.

DOPE-Rhod was used for fluorescence detection. Images were acquired after the liposome/lipoplex immobilization procedure was finished. Results are presented in Figure 3.2.

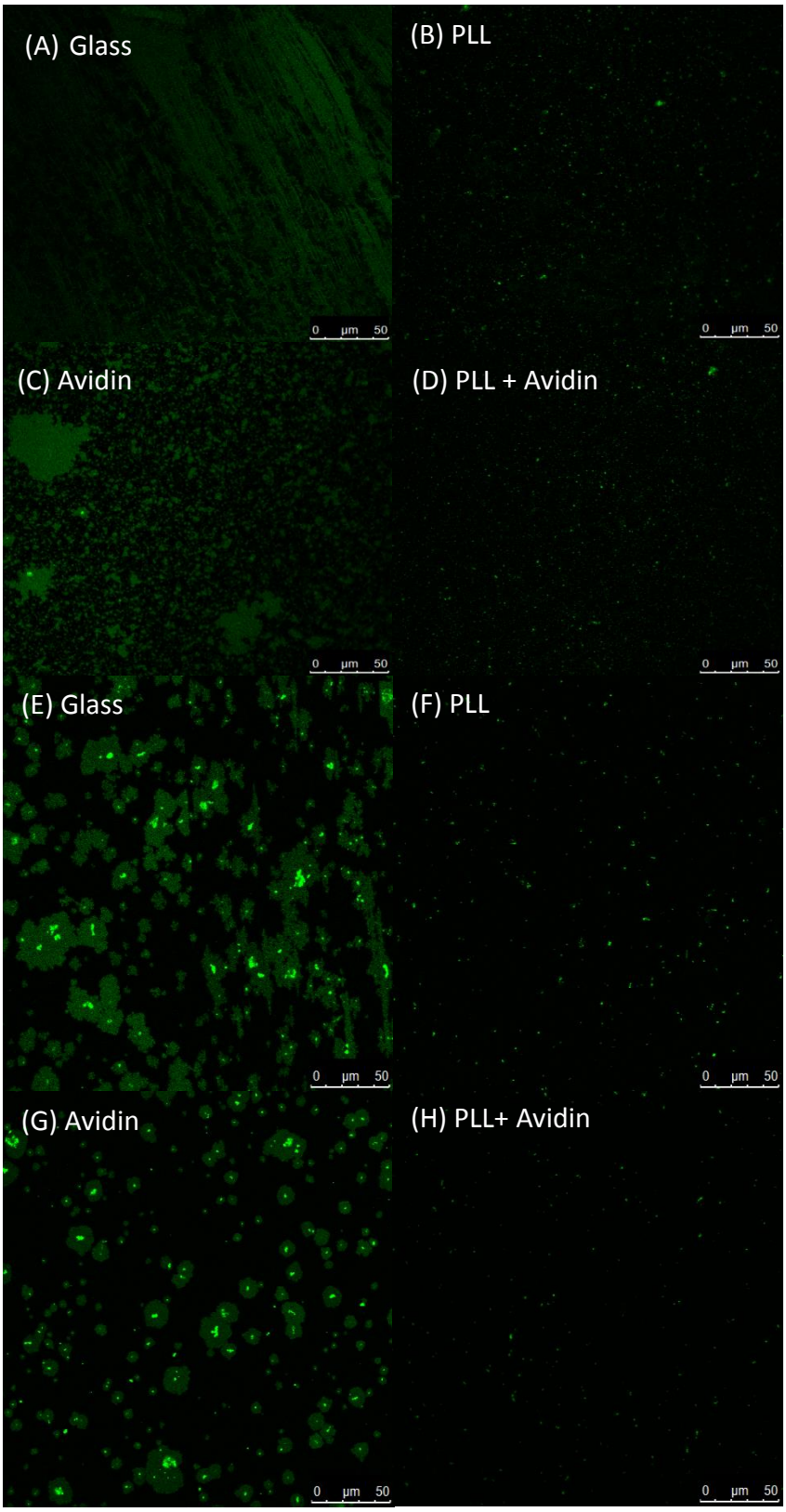

Figure 3.2 Test for immobilization of liposomes (A)-(D) and lipoplexes (E)-(H) imaged through DOPE-Rhod fluorescence Lipoplexes (where pDNA was used) are significantly brighter than liposomes without pDNA. Conditions where no coating or only avidin were used (on the left) led to collapse of vesicles and formation of SLB's

In general, in the conditions where liposomes alone were tested, liposomes were immobilized at very high densities and were considerably less bright than lipoplexes, although brightness was highly variable. This is a result of liposome fusion observed in the presence of DNA which leads to the formation of larger and brighter particles[32].

Incubation of liposomes/lipoplexes on both glass and avidin surfaces led to the formation of planar supported lipid bilayers (SLB). The formation of this structure does not require immobilization as it is observed even in the absence of avidin, and is due to the collapse of vesicles in the glass surface, likely due to electrostatic attraction for the negatively charged glass surface. On the other hand, PLL coating largely eliminates SLB formation and liposomes/lipoplexes can be visualized as discrete units, although liposomes are found at very high densities. This is likely due to electrostatic repulsion between cationic liposomes/lipoplexes and the also positively charged PLL coated surface, which is likely to inhibit liposome collapse in to the surface. It should be noted that liposome/lipoplex adhesion to the PLL coated surface is also observed in the absence of avidin, However, in the presence of avidin, the surface distribution of liposomes is much less homogeneous, suggesting a higher efficiency of liposome immobilization in avidin+PLL coated surfaces, as expected. A larger fraction of smaller lipoplexes are also observed in the presence of avidin suggesting that biotin-avidin ligation allows for a more efficient immobilization of small lipoplexes, while immobilization in a PLL surface in the absence of avidin is much more effective for larger particles.

The fact that coating proteins stabilize lipoplexes has been investigated and is known to increases transfection efficiency and decrease the amount of DNA needed for efficient transfection to occur [94].

3.3. Reverse Lipofection Exploratory Assays

Initial assays for reverse transfection have been previously done in our lab. In these assays, total lipid concentration was 500-fold higher but showed a high cytotoxicity (results not shown). In this sense it was decided to start the assays with much lower concentrations. Regardless of this observation, no cytotoxicity tests were further performed and only transfection efficiencies were taken into account throughout this work.

Furthermore different DOTAP: DOPE proportions were tested: 1:1; 1:3 and 3:1. The influence of PLL coating was also tested and SUV's were used at three different lipid concentrations: 3.6, 7.2 and 14.4 ng/µL. pDNA concentration was established at 2ng/µL. The results were obtained by confocal/multiphoton microscopy and are presented in Figure 3.3.

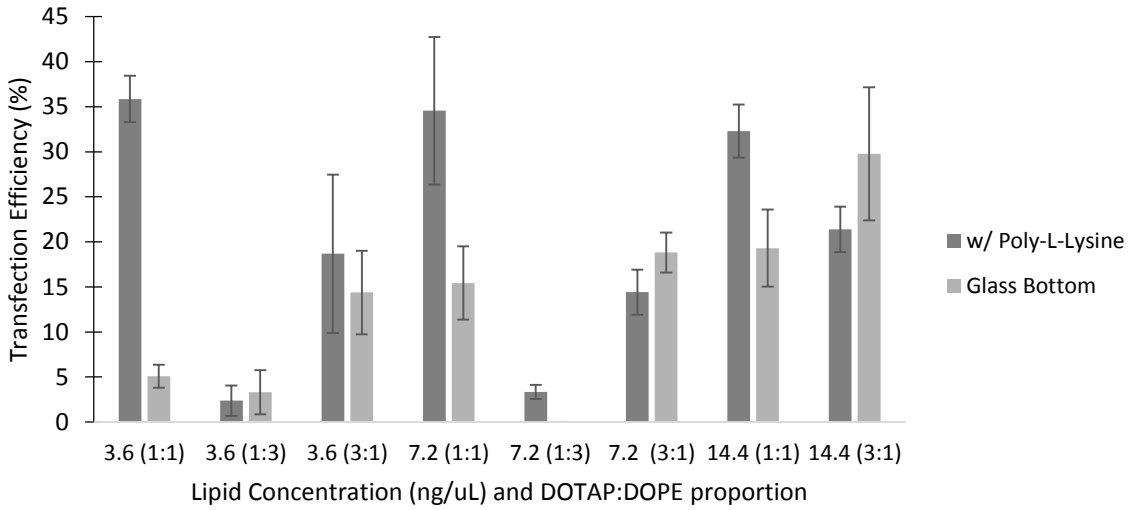

Figure 3.3 Transfection efficiency in IBIDI chambers with no coating (glass bottom) or with PLL coating. Different lipid concentrations and DOTAP: DOPE proportions were tested. Results for DOTAP:DOPE proportion 1:3 at 14.4ng/µL were not collected. Error bars represent standard deviation values. (Results from Confocal/Multiphoton microscopy)

In general, the conditions that had PLL showed higher transfection comparing to the similar ones without PLL. Nevertheless this effect seems to decrease with increasing concentrations of lipid.

The conditions that showed higher transfection efficiencies (36, 35 and 31%) were for 3.6, 7.2 and 14.4 ng/µL of lipid, respectively, in a DOTAP:DOPE proportion of 1:1, with PLL. This shows that regardless of the concentration, the proportion 1:1 show similar transfection efficiencies when using PLL. In addition the maximum concentration for the DOTAP:DOPE proportion 3:1 without PLL showed a similar efficiency (30%).

In the previously presented assay, a plasmid DNA purified by Hydrophobic Size Exclusion Chromatography was used (Hic-Sec) as described by Diogo et al (2005)[89]. Since a new plasmid batch was produced (as described in Materials and Methods) it was necessary to test it and compare with the previous one. Also a plasmid purified by a MiniPrep Kit was included in the assay.

Additionally, a change from glass substrate to plastic surfaces was predicted: in the second part of this work, a higher number of cells was needed to perform flow cytometry, and so 24-well plates were used instead of IBIDI chambers. In this sense, it was necessary to test if the transfection efficiency in a material similar to the one of 24-well plates was comparable to the one obtained in glass substrates.

So, besides testing the impact of plasmid purification method, Uncoated IBIDI chambers with polymer coverslips (instead of glass) were tested. In both situations, the experimental conditions were: PLL coating, lipid concentration of 7.2 ng/µL, SUV's at 3:1 and 1:1 DOTAP: DOPE proportion and pDNA concentration of 2 ng/µL. Results were obtained by Confocal/Multiphoton Microscopy and are presented in Figure 3.4.

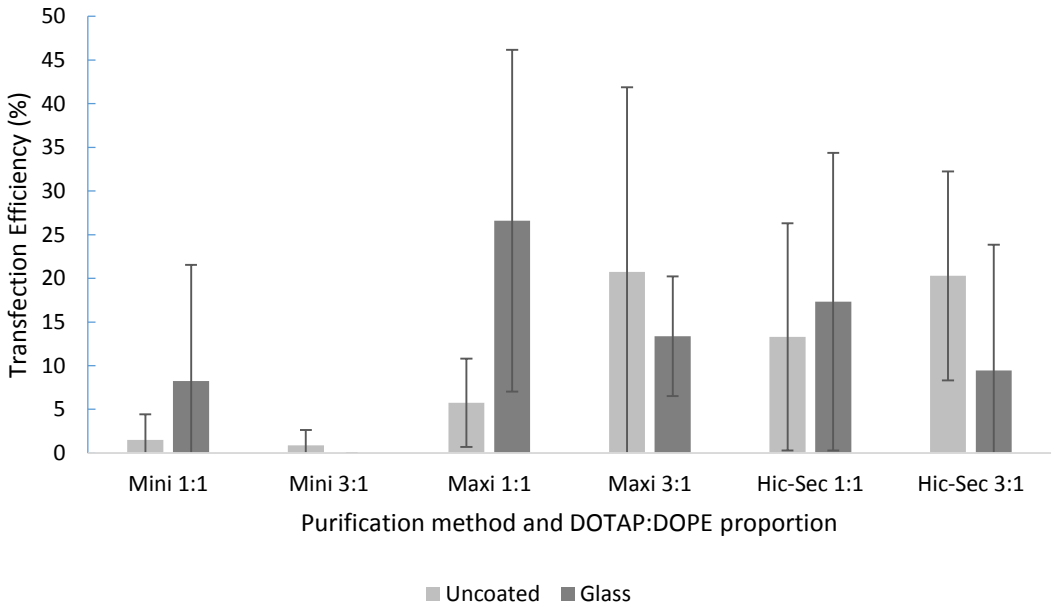

Figure 3.4 Transfection efficiency in both IBIDI glass chambers and uncoated chambers. pDNA from three different purification methods were tested: MiniPrep, MaxiPrep and Hic-Sec purification. Also, two different DOTAP:DOPE proportions were tested. Error bars represent standard deviation values. (Results from Confocal/Multiphoton microscopy)

As expected, plasmids purified with the MiniPrep kit showed lower transfection efficiency. This result was expected since pDNA purified by this kit also contains gDNA and endotoxins as observed by La Vega et al (2013) that might impair transfection efficiency[95].

Both Maxi and Hic-Sec methods showed comparable transfection efficiencies: mean transfection values, regardless of the other conditions, were 17% for Maxi and 15% for Hic-Sec. In addition, mean transfection efficiencies for the different substrates were also comparable: with 15% for polymeric coverslip and 17% for glass. In this way, one can conclude that there is no significant difference between using plasmids obtained from Maxi or Hic-Sec, and between polymeric and glass substrates.

The large standard deviations obtained for transfection efficiency at each condition is likely inherent to the quantification of the fraction of transfected cells by microscopy, as only a minor fraction of the population is assessed, and the transfection efficiency is highly non-uniform within each well. In this way, when dealing with large amounts of data and when high throughput results are desired this analysis method is not efficient.

3.4. Reverse Lipofection Optimization

3.4.1.Experimental Design

From the results from the previous sections it is not possible to draw strong conclusions of how this method should be applied. Furthermore, when testing several conditions simultaneously it is impossible to predict

what factors are generating the variations observed. On the other hand, varying each factor at a time is time consuming and requires a massive number of experiments. Also, when varying a variable at a time, the dependence between the variables is neglected.

In this context, Response Surface Methodology (RSM) was used for the optimization of the proposed technique: the factors under study were combined at different levels to evaluate the influences and interactions between the variables affecting the response. Each variable was studied at three different levels. In the context of this methodology they are called the independent variables. The transfection efficiency is the response variable.

Five different variables were studied: total lipid concentration, DOTAP:DOPE proportion, liposome size, pDNA concentration and initial number of cells The first four variables are known to influence lipoplex size, shape and charge, the way lipoplexes interact with cells and ultimately the gene delivery capacity. Regarding cell confluence, the physiological state of the cells plays a major role in defining the efficiency of gene delivery.[33] It is well established that gene deliver depends on cell cycle[96]. Since in this work lipoplexes are available for transfection throughout the whole experiment and cell division is likely to occur, different initial number of cells were tested.

The first step was to choose an appropriate design within the experimental region under study. The design chosen was a Central Composite Face Centered Design (CCF). It allows for a quantitative estimation of effects and interactions of each variables on the transfection efficiency by measuring the differences on the response variable as the independent variables are changed from low (-1) to high (+1) values.

The following table represents the maximum obtained for each set of assays and respective assay. It is also represented the average transfection efficiency obtained in each set of the 30 assays.

Table 3.1 Average transfection efficiency, maximum transfection efficiency and respective assay for each set.

Set	**1**	**2**	**3**	**4**
Set Average Transfection Efficiency	2.89	6.11	2.67	9.87
Assay w/ Maximum Transfection Efficiency	13	23	13	14
Maximum Transfection Efficiency	6	22.43	10.7	63.32

Table 3.2 represent the design of the assays performed and the results. Results presented are for mean of replicates. Four sets of replicates were performed for the 30 assays and in each set, results were normalized to the value of maximum transfection efficiency within each set.

Figure 3.5 shows the average relative transfection efficiencies and standard deviations for each of the conditions. The bars are for standard deviation. It should be noted that because of the differences between replicates the values took into account for the building of the model were the mean values of replicates.

Table 3.2 Experimental design based in a CCF design and replicates mean for relative transfection efficiency

Assay	X_1	X_2	X_3	X_4	X_5	Transfection Efficiency
1	-1	-1	-1	-1	1	0.07
2	-1	-1	-1	1	-1	0.05
3	-1	-1	1	-1	-1	0.29
4	-1	-1	1	1	1	0.13
5	-1	1	-1	-1	-1	0.52
6	-1	1	-1	1	1	0.11
7	-1	1	1	-1	1	0.29
8	-1	1	1	1	-1	0.12
9	1	-1	-1	-1	-1	0.21
10	1	-1	-1	1	1	0.18
11	1	-1	1	-1	1	0.14
12	1	-1	1	1	-1	0.13
13	1	1	-1	-1	1	0.72
14	1	1	-1	1	-1	0.83
15	1	1	1	-1	-1	0.51
16	1	1	1	1	1	0.26
17	-1	0	0	0	0	0.20
18	1	0	0	0	0	0.48
19	0	-1	0	0	0	0.18
20	0	1	0	0	0	0.17
21	0	0	-1	0	0	0.12
22	0	0	1	0	0	0.15
23	0	0	0	-1	0	0.51
24	0	0	0	1	0	0.24
25	0	0	0	0	-1	0.25
26	0	0	0	0	1	0.16
27 (C)	0	0	0	0	0	0.22
28 (C)	0	0	0	0	0	0.21
29 (C)	0	0	0	0	0	0.20
30 (C)	0	0	0	0	0	0.35

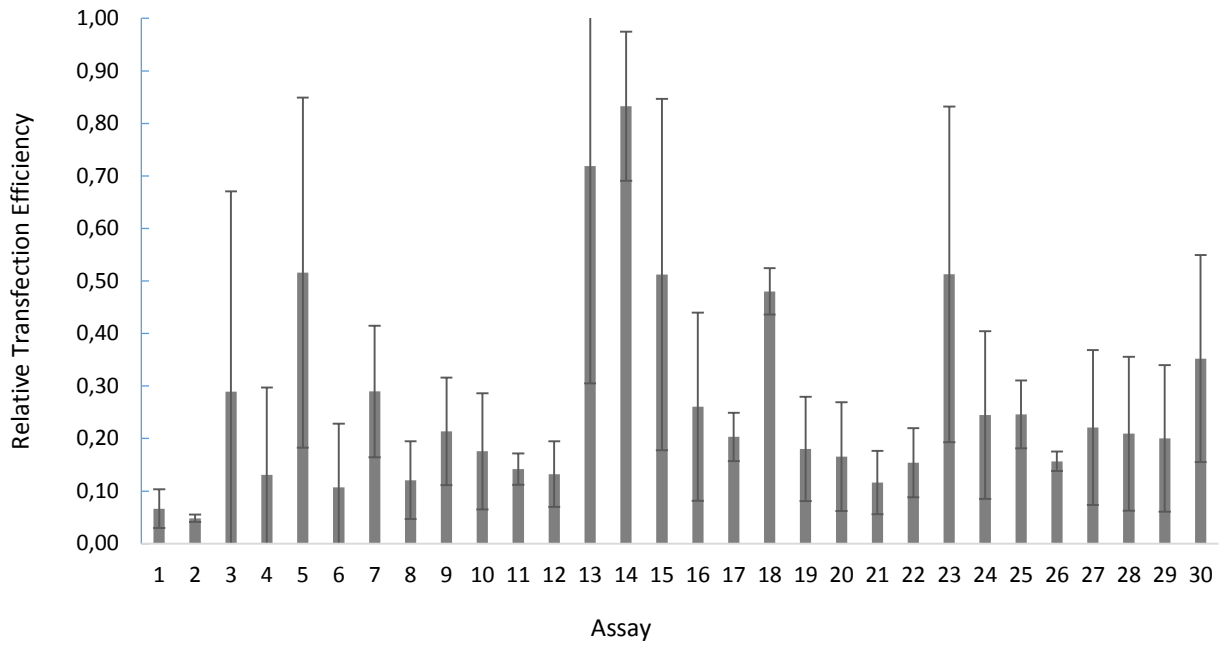

Figure 3.5 Graphical representation of the relative transfection efficiency obtained for each assay. Error bars represent standard deviation

These assays were performed in 24-well plates, which is in fact a different material than the previous used for lipoplexes immobilization testing. To overcome this issue it was first tested the use of glass coverslips on the bottom of the wells so the surface would be comparable to previous experiments. To avoid growth of cells on the surrounding plastic a thin layer of 3% agarose would be deposited prior to the application of the coverslip. Also, coverslips were previously washed with Tween 80 in ultrasound bath to eliminate fats and dust particles. In fact, the use of agarose limited the growth of cells to the glass coverslip, but this technique proved to be ineffective since it is impossible to control in which side of the glass coverslip the cells will attach. Furthermore, it is very difficult to detach the cells from the slides, which is a major disadvantage when a maximum number of cells is desirable to carry out flow cytometry. Nevertheless, it should be noted that this technique might be very effective for transfecting cells in coverslips for use in microscopy applications.

The reverse lipofection technique was therefore directly applied on the polystyrene wells. The primary PLL coating and the stabilization effect that it seems to have on lipoplexes is likely to mitigate potential differences observed for glass or polystyrene. Furthermore, given the ubiquity of polystyrene in cell culture materials, results obtained with this material are of great significance and more readily reproducible in different supports.

Although in general, the transfection efficiency values are low and far from an ideal transfection efficiency, differences between conditions can be perceived and for that reason it is possible to analyze the impact of each factor on transfection efficiency and the dependence between different factors.

3.4.2.Model Building

Before model building, the first step was to determine the effect estimates for each factor. This represents the improvement in the response variable that is to expect as each variable setting is changed from low to high. This can be visualized in the Pareto chart present in Figure 3.6. In this chart, the absolute value of magnitude of the standardized effect estimate (i.e. the effect estimate divided by the corresponding standard error) is represented for each factor (linear and quadratic effect) and for the interaction between factors sorted by their absolute sizes. Each factor or interaction is also compared to the 95% confidence minimum for statistical significance (represented by the dashed line that set p=0.05).

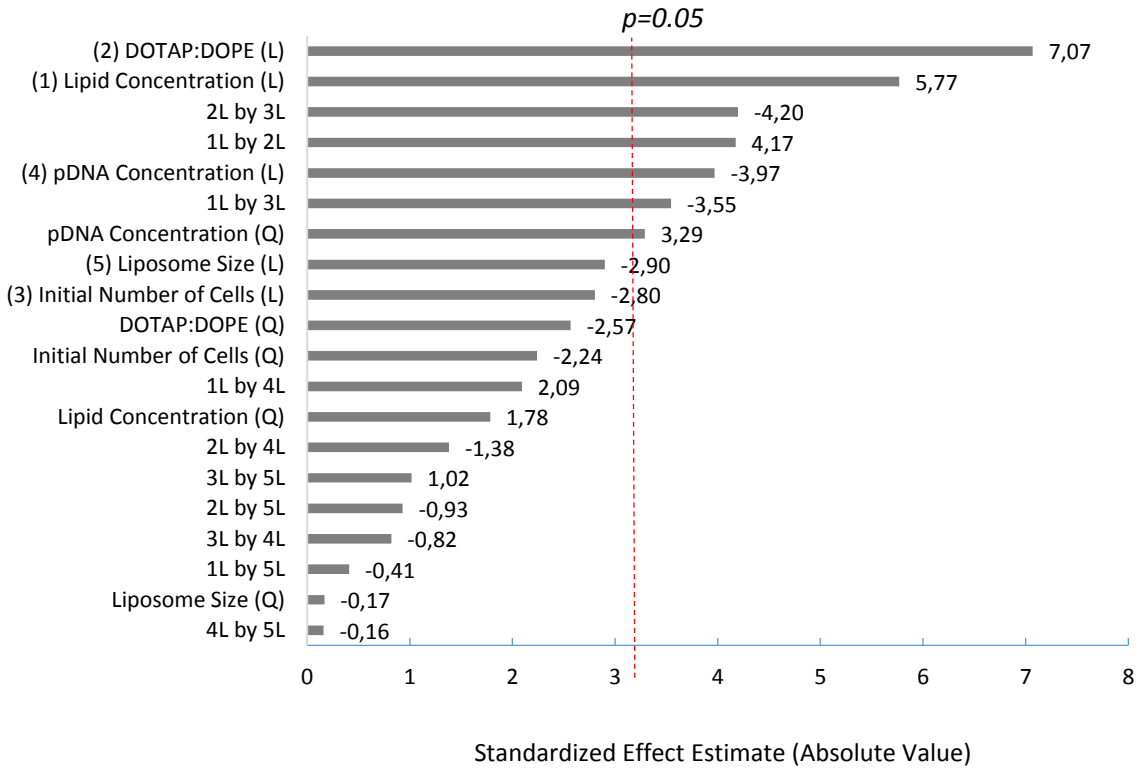

Figure 3.6 Pareto Chart of standardized effects estimates obtained for the response variable. Dashed line for a confidence of 95% which corresponds to an F-value of 3.18. Effects that do not cross 95% confidence were removed and pooled into error term (except for the linear effects of liposome size and initial number of cells)

Factors and interactions that were not statistically valid (meaning the ones that not cross the 95% confidence threshold) were removed and pooled into the error term. The exceptions were the linear effects of liposome size and initial number of cells, so all linear effects of each variable would be included in the model to avoid possible inconsistent results during optimization. Furthermore, initial number of cells plays a great effect in interaction with DOTAP: DOPE proportion.

Quadratic effects (except for pDNA concentration) and interactions 1L by 4L (lipid concentration x pDNA concentration), 2L by 4L (DOTAP:DOPE proportion x pDNA concentration), 3L by 5L (initial number of cells x liposome size), 2L by 5L (DOTAP:DOPE proportion x liposome size), 3L by 4L (initial number of cells x

pDNA concentration), 1L by 5L (lipid concentration x liposome size) and 4L by 5L (pDNA concentration x liposome size) were removed and pooled into the error term.

According to Figure 3.6, the factor that has the greatest effect on the transfection efficiency is DOTAP:DOPE proportion (7.07) followed by lipid concentration (5.77). Both factors have a positive effect meaning that increments in these variables results in an increase in the response variable. On the other hand, the interaction between DOTAP:DOPE proportion and the initial number of cells, together has a negative effect on the response variable (-4.20). This is expected if one takes into account the negative effect of initial number of cells alone (-2.24). Similarly, the interaction between DOTAP:DOPE proportion and lipid concentration has a positive effect on the response variable. It should also be noted that pDNA concentration has a negative effect on the response variable (-3.97). Lower values for this variable promoted a higher transfection efficiency.

The response variable was then expressed as a function of the independent variables that were included in the model. The model coefficients were estimated by a least square fitting to the experimental results.

$$\%\, Transfection =$$
$$= -0.083243(\pm 0.135304) + 0.092405(\pm 0.028239)X_1 + 0.152121(\pm 0.046035)X_2 +$$
$$0.000017(\pm 0.000005)X_3 - 0.120291(\pm 0.045121)X_4 - 0.0003(\pm 0.000092)X_5 + 0.018214(\pm 0.009618)X_4^2 +$$
$$0.026218(\pm 0.006179)X_1X_2 - 0.000004(\pm 0.000001)X_1X_3 - 0.000006(\pm 0.000002)X_2X_3$$

3.4.3.Model Validation

The statistic validation of the reduced model was conducted by means of analysis of variance (ANOVA) as described in Materials and Methods. Since experimental data was replicated at central point pure error from experimental replication can be estimated and estimation of the LOF is possible. This allows the comparison between residual error to pure error from replication.

F-values and p-values for the model, error and LOF are summarized in Table 3.3.

Table 3.3 ANOVA outcome for the reduced model showing the three main sources of variation including discrimation of the pure error and lack of fit

Source	SS	df	MS	F-value	p-value
Model	0.85	9	0.09	18.43	0.01770
Error	0.21	20	0.02		
Lack-of-Fit	0.19	17	0.01	2.23	0.27882
Pure Error	0.02	3	0.01		
Total	1.06	29			

By observation of the table, one can conclude that the model is statistically valid (p-value|Model < 0.05, 0.01770) and explains 79% of the observed variance (R^2 = 0.7987). In addition, there is no evidence of LOF

at the 95% confidence level (p-value|LOF >0.05; 0.27882), meaning that the model is explaining the observed differences in the response variable.

3.4.4.Optimization

The relationship between variables and response can be easily visualized by means of RSM. Based on the mathematical model previously presented, response surfaces were generated by representing the response variable as a relation of two independent variables. The three other variables not presented in the graphs were fixed. Although these observations are empirical, several correlations between the variables can be identified.

Liposome size was one of the variables that had a smaller effect on the response variable. Additionally, none of their interactions with other variables was statistically significant. This observation may be consistent with observations from Ross et al (1999)[49] that although liposomes are prepared before complexation with DNA, transfection activity is only dependent on the final size of the complexes and not on the size of the liposomes used. To confirm this, measurements of the size of liposomes before and after complexation with DNA should be performed.

Liposome size have a negative effect on the response variables, meaning that the lower value for this variable promoted higher transfection efficiencies. For this reason, in the next analysis here presented, liposome size was set to 50nm.

Nevertheless, it should be noted that at high lipid concentrations, the decrease of transfection efficiencies with increasing liposome sizes became less significant, since transfection efficiency with 100 and 400 nm liposomes are comparable to transfection efficiencies measured with smaller liposomes. This is particularly evident when lower numbers of cells are used. The following graphs illustrate these observations.

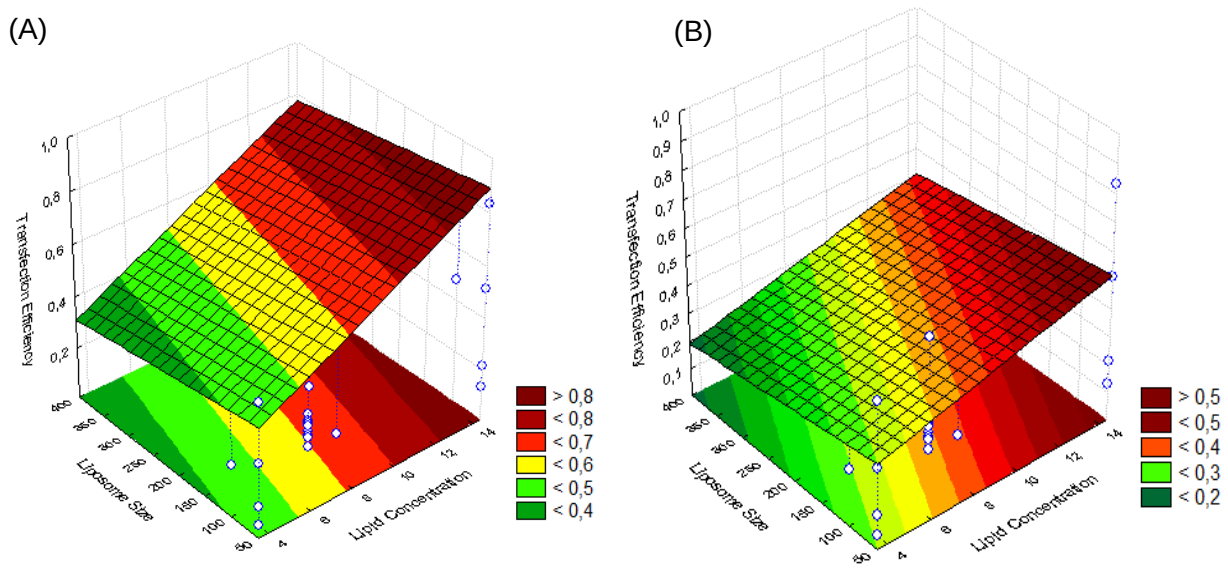

Figure 3.7 Effect of liposome size and lipid concentration on relative transfection efficiencies when low (17000 cells/cm^2) (A) and higher (34000 cells/cm^2) (B) initial number of cells are used. pDNA concentration was set at 1ng/µL and DOTAP:DOPE proportion to 3. Notice, especially in the first graph, that at high lipid concentrations, transfection efficiency with 100 and 400 nm liposomes is comparable to the transfection efficiency of 50nm liposomes.

The initial number of cells also had a limited (not statistically valid) impact on transfection efficiencies. But in opposition to the previous discussed variable, two of its interactions (with the proportion of DOTAP:DOPE and with lipid concentration) were statistically valid. Both interactions have a negative effect in transfection efficiency and both might be explained by cytotoxicity of cationic lipids. In this context, assays where higher proportions of DOTAP were used added with the higher lipid concentrations promote higher levels of toxicity. Still, experiments carried out with a lower fraction of DOTAP and lower lipid concentrations, promoted lower transfection efficiencies, despite lower levels of cationic-lipid related toxicity.

The toxicity of cationic lipids is well-established and was previously referred in Introduction of this work[33].

The following graphs illustrate the previous observations. Liposome size was set to 50 nm and pDNA concentration at 1ng/µL. Lipid concentration was gradually increased.

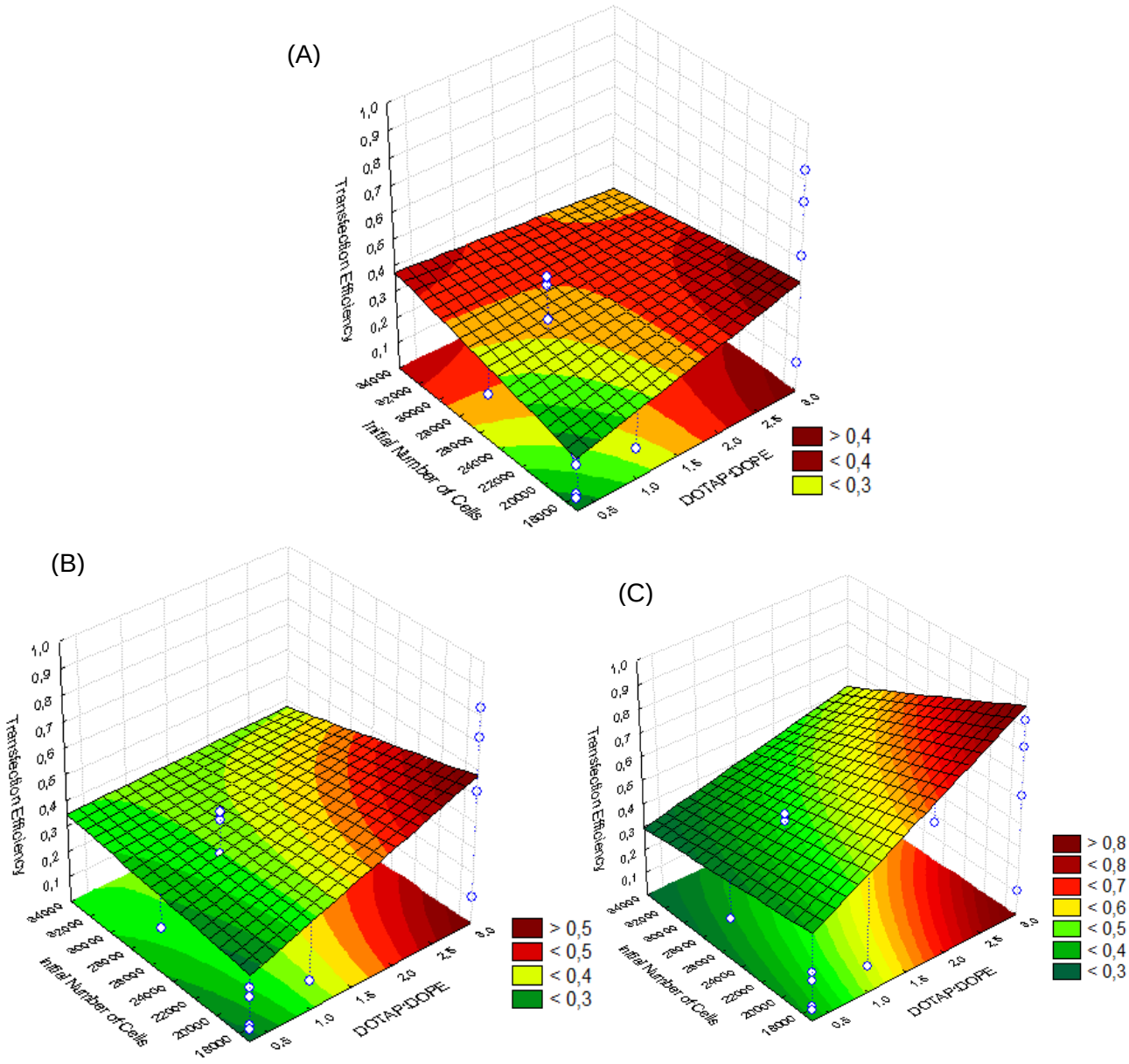

Figure 3.8 Effect of initial number of cells and DOTAP:DOPE proportion on relative transfection efficiencies as lipid concentration is increased: 3.6ng/µL (A), 7.2 ng/µL (B) and 14.4ng/µL (C). pDNA concentration was set to 1ng/µL and liposome size to 50nm. A low initial number of Cells promote higher transfection efficiencies but lipid concentrations plays a major role in this effect, as when lipid concentrations decrease, a higher initial number of cells promote a relative transfection efficiency comparable to the one obtained with a low number of cells.

In this sense, it can be seen that when higher lipid concentrations are used, higher transfection efficiencies were obtained with lower cell numbers. Nevertheless, when lipid concentrations are lowered, a higher cell number is more advantageous. Nevertheless, the first situation promotes the highest transfection efficiency observed.

Furthermore, it is well established that actively dividing cells promote higher cationic liposomes gene delivery[97,98]. Taking this into account it might be expected that a low Initial Number of Cells promote cell division and hence higher gene delivery. Thermo Fisher proposed protocol for Lipofectamine ® 2000 (https://www.thermofisher.com/pt/en/home/references/protocols/cell-culture/transfection-protocol/lipofectamine-2000.html) suggests the plating of 25000-62500 cells/cm^2 the day before transfection so an optimum result can be obtained. In the case of this work, plating fewer cells at the time of transfection promoted the best results.

One can go into higher detail in the interaction between the proportion of DOTAP:DOPE and lipid concentration. These isolated variables have the greatest impacts in the response variable and their interaction has the fourth greater effect. Also, pDNA concentration will be discussed along DOTAP:DOPE and lipid concentration. Since these 3 factors together influence lipoplex stability and transfect efficiency, it makes no sense to discuss them separately.

Generally the impact of both higher DOTAP:DOPE proportion and lipid concentration is positive, meaning that higher values for both variables promote higher transfection efficiency. Regarding the first variable, this result was expected because in conditions where an excess of zwitterionic lipid is used, complexation with pDNA is impaired, or complexes are actually formed but not stable and pDNA becomes susceptible to degradation. This evidence can be observed in Figure 3.8 (B) and (C), where relative transfection efficiencies over 0.4/0.5 only occur with DOTAP:DOPE proportions above 1. On the other hand, when an excess of cationic lipid is present, it forms more stable complexes with DNA. These observations are easily identifiable in Figure 3.9.

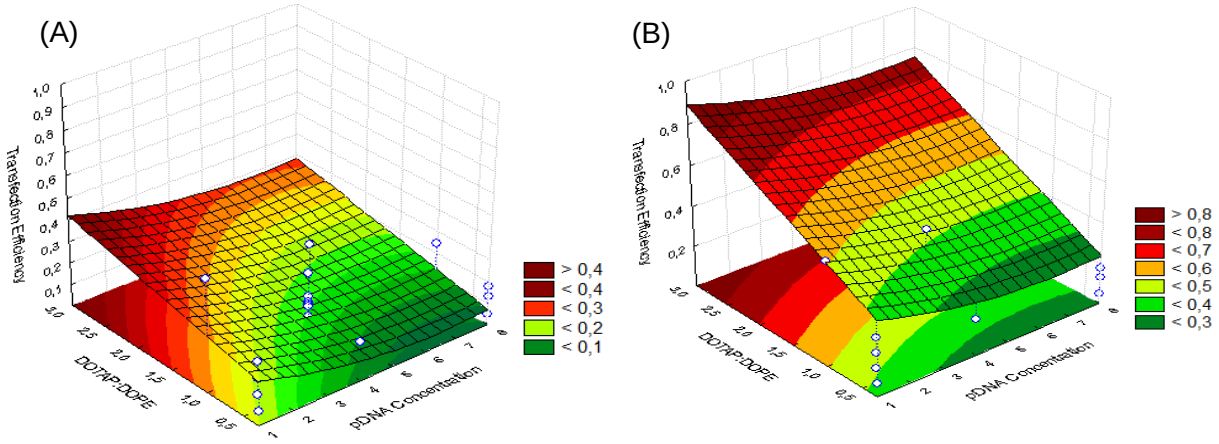

Figure 3.9 Effect of DOTAP:DOPE proportion and pDNA concentration on relative transfection efficiency as Lipid concentration is increased from 3.6ng/µL (A) to 14.4ng/µL. Initial number of cells and liposome size values were set to 17000 cells/cm^2 and 50nm, respectively. When Lipid concentration increases the impact of pDNA concentration is limited.

Regarding maximum transfection efficiency, three main observations can be withdrawn from these graphs: (1) higher transfection efficiencies were observed at the highest lipid concentrations and DOTAP:DOPE proportions used, (2) higher pDNA concentration lead to a decrease in transfection efficiencies (3) In the presence of higher lipid concentrations the impact of the other variables is mitigated. The last observation is particularly clear in Figure 3.9 (B) where higher pDNA concentrations led to a transfection efficiency comparable to the one promoted by lower concentrations. This is likely to occur because an optimum range (for transfection) of lipid/DNA ratio exists, and at high lipid concentrations this ratio is always within this range, unlike what is observed in the presence of lower lipid concentrations, where the lipoplexes are saturated with DNA, decreasing their efficiency. Interestingly, and in contrast to what has been previously observed, when using a high initial number of cells and low lipid concentration, a DOTAP:DOPE proportion of 1:3 promoted higher transfection efficiencies as depicted in Figure 3.10.

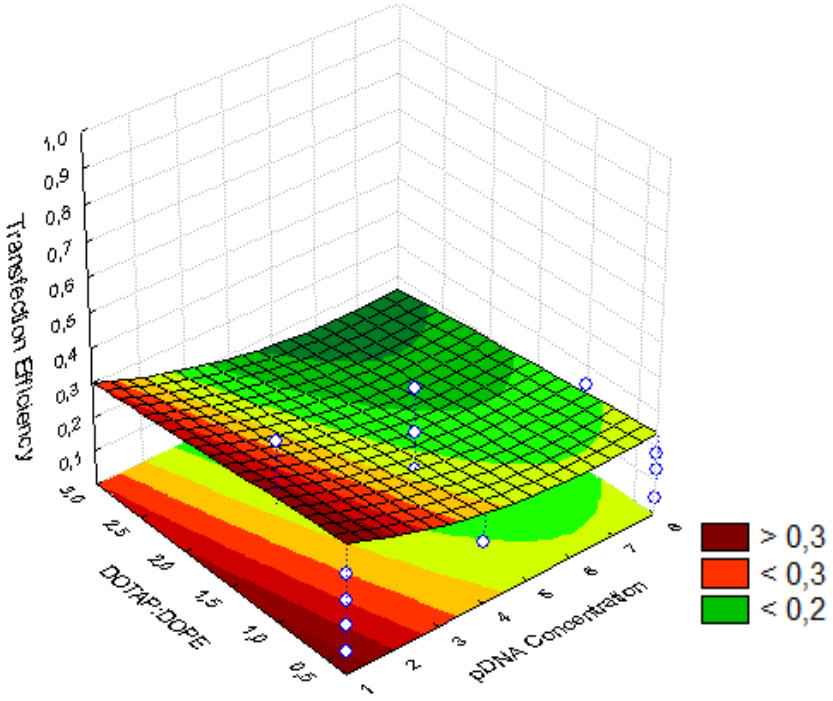

Figure 3.10 Effect of DOTAP:DOPE proportion and pDNA concentration on the transfection efficiency when a high Initial number of cells (34000 cells/cm^2) and low lipid concentrations (3.6ng/µL) are used. In opposition to what was previously observed, liposomes with a 1:3 DOTAP:DOPE proportion are the most efficient transfection vehicles

Nevertheless, since relative transfection efficiencies in these conditions are low (lower than 0.5). The mechanisms responsible for this difference were not further explored.

3.5. Further Considerations

Much of the behavior here discussed might be explained by the charge ratios (+/-) of the lipoplexes, which were previously calculated and presented in Table 2.2. A neutral charge ratio (+/-) is typically avoided because it results in the formation of large aggregates (>1µm). Lipoplexes prepared at positive and negative charge ratios likely represent structures with different lipid-DNA and DNA packaging[90]. Additionally charge ratios have a major impact in lipoplex size as previously referred in Introduction and reviewed by Zhang et al (2012)[50]

Madeira et al. (2007), observed by gel retardation assays that at a given lipid concentration, for lipoplexes without DOPE at charge ratios (+/-) of 4 and 6 there were still free pDNA molecules, but by including DOPE in the lipid mixture, the DNA became fully protected at charge ratios (+/-) down to 2. This system is comparable with the one used in this work, since pDNA is the original pVAX with LacZ. For lipoplexes (with both DOTAP and DOPE) with charge ratios (±) ≥4, the pDNA complexation efficiency was 100%. For lower charge ratios (+/-), DNA complexation efficiency decreased to 94 and 30% for charge ratios (±) of 4 and 0.5, respectively.

As can be seen in Table 2.2 lipoplexes charge ratios (+/-) used in this work vary from 0.05 to 4.99 meaning that the majority of the lipoplexes used are far from the ideal 100% complexation efficiency. In fact, for example Assay 13 presents a charge ratio (+/-) above 4: lipid concentration= 14.4ng/µL; pDNA concentration=1ng/µL and DOTAP:DOPE proportion of 3:1. Although some of the highest transfection efficiencies were observed for this sample, the lipoplex charge ratios were not the most important factor in dictating transfection success, since the highest transfection efficiency (63.3%) was observed for assay 14, where the lipoplex charge ratio (+/-) was 0.62. Assays 13 and 14 had in common the same lipid concentration (14.4ng/µL) and lipid composition, and were obtained for the same initial concentration of cells (17000 cells/cm^2), while the DNA concentration differences accounts for the different charge ratios. This suggests that lipid concentration is a much more important predictor of transfection efficiency than the charge ratio. However, it is unclear if this is due solely to an increase in lipoplex numbers, or to the importance of the total lipid concentration (independently of DNA concentration) in defining the extent of DNA complexation, or alternatively if it is due to more sophisticated mechanisms occurring during intracellular lipoplex trafficking.

Although charge ratios are clearly not the crucial parameter in defining transfection efficiency, they do seem to correlate with transfection efficiency to some extent. Since the majority of the lipoplexes used had a charge ratio (+/-) ≤1 it is possible that the optimization presented here did not fully cover the expected variable space of maximized transfection efficiencies. From the RSM plots obtained this can also be concluded. The following image illustrates this observation.

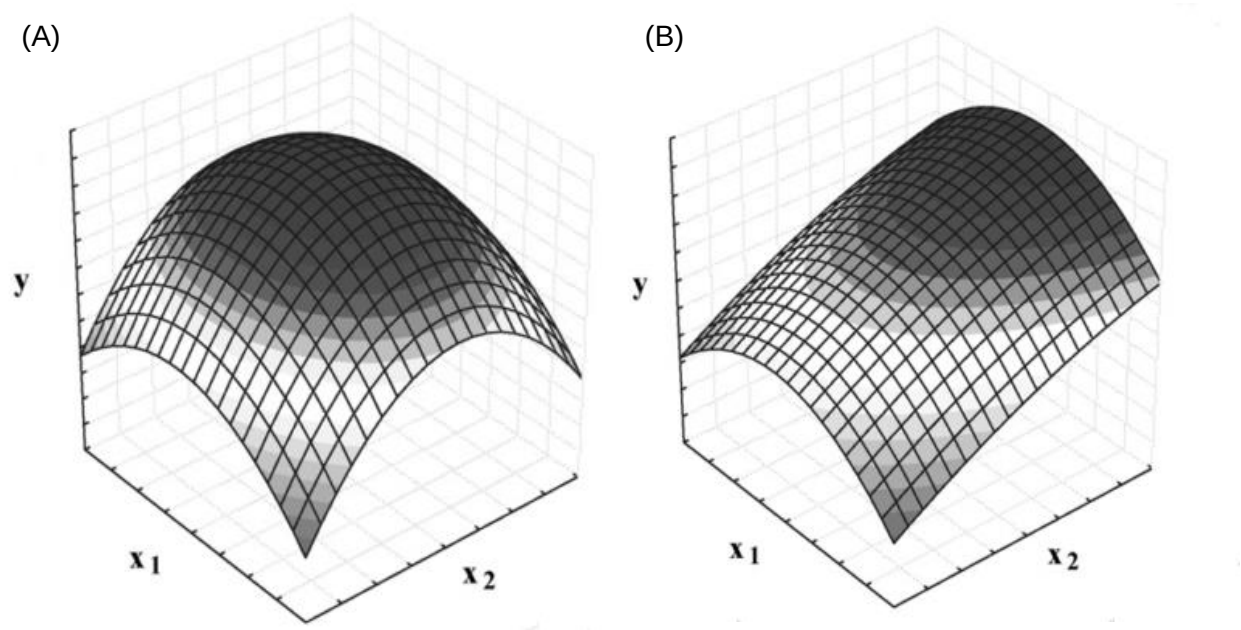

Figure 3.11 RSM graphs showing an optimum inside the experimental region (A) and a result suggesting an optimum outside the experimental region (B). Y is for the response variable and X_1 and X_2 for hypothetical independent variables.The graphs obtained in this work are more similar to the second situation (Adapted from Bezerra et all (2007)[83]

The SRM plots obtained in this work are more similar to the one presented in situation (B). Figure 3.11(A) shows a situation where the variable space of maximized response is inside the experimental variable space under study. In the second situation, the variable space of maximized response is outside the variable space studied. Establishing a relation between these graphs and the ones obtained in this work, and taking into account the previous observation regarding charge ratios (**+/-**) one can affirm that the experimental region under study in this work is far from the ideal.

4. CONCLUDING REMARKS AND FUTURE WORK

Gene therapy is still in its infancy and much research is still to be done. Several mechanisms underlying gene delivery are still poorly understood which are preventing gene therapies to move forward to more clinical trials.

Several mechanisms at the cell level are to be understood, especially concerning endosomal escape, cytoplasm movement and nuclear delivery. Nuclear delivery in particular is the critical barrier for efficient gene delivery to non-dividing cells.

In this work, a new reverse lipofection assay was proposed and developed. The novelty of this methodology is the combination of cationic lipid-mediated gene delivery with intact lipoplexes and a reverse transfection approach, which could potentially offer the combined advantages of both technologies, namely high transfection efficiencies, the possibility of spatially defined transfection, as well as increased success in transfection of hard to transfect cell lines (as previously observed in other reverse transfection approaches).

Here, we focused on the optimization of transfection efficiencies. As a new reverse lipofection method and regarding transfection efficiency, expectations were exceed, since 63.3% transfection was achieved in some conditions. But some work is still required to guarantee reproducibility of the results. RSM assays showed that higher transfection efficiencies are expected for higher lipid concentrations at the highest DOTAP:DOPE proportion tested, (3:1). Liposome size had limited impact and a lower Initial Number of Cells promoted higher transfection efficiencies. Higher pDNA concentrations limited transfection efficiencies at low lipid concentrations, but only had a small effect in the presence of higher lipid content.

RSM proved to be a crucial tool in this work. As an optimization tool it was possible to estimate the effect of each variable in the response variable and above all it was possible to understand the relationship between independent variables that wouldn't be possible with conventional one-variable-a-time optimization. Ultimately it was possible to perceive that the experimental region under study might be outside the optimum region in what concerns the transfection efficiency. This is particularly evident for the relation between lipid concentration and pDNA concentration (translated in charge ratio (**+/-**), as mostly low charge ratios were explored. In this sense, future optimization work must consider the change of the experimental region under study in a way where higher lipoplex charge ratios (**+/-**) are considered. However, is highly likely that increasing lipid concentration will compromise cell viability to some extent. In this context, cytotoxicity assays are needed to prove that an increase in lipid concentration would not be excessively toxic for the cells. Also, cytotoxicity assays are needed for a better understanding of the impact of DOTAP:DOPE proportion on cell viability, as well as on the mitigation of toxicity by the presence of a higher initial number of cells

Finally, once the reverse lipofection method itself is optimized, one can go further into spatially defined transfection. Since the avidin-biotin system has proven to efficiently immobilize lipoplexes, it is possible to

create a surface differentially coated with avidin that spatially immobilizes lipoplexes by means of, for instance, photolithography. Such a system may also be very useful in microfluidics devices and in cell array technologies.

5. REFERENCES

1. Zhao, Q.,Chen, J, Lv, T., He, C., Tang, G., Liang, W., Tabata, Y., Gao, J. N/P ratio significantly influences the transfection efficiency and cytotoxicity of a polyethylenimine/chitosan/DNA complex. *Biological and Pharmaceutical Bulletin* **32,** 706–710 (2009).

2. Segura, T., Shea, L. D. Surface-Tethered DNA Complexes for Enhanced Gene Delivery. *Bioconjugate Chemistry* **13,** 621–629 (2002).

3. Gao, X., Kim, K., Liu. D. Nonviral gene delivery: what we know and what is next. *The AAPS Journal* **9,** 92-104 (2007).

4. Gene Therapy Clinical Trials Worldwide. at <http://www.wiley.com/legacy/wileychi/genmed/clinical/>(Acessed October 2015)

5. Kim, T. K., Eberwine, J. H. Mammalian cell transfection: the present and the future. *Analytical and Bioanalytical Chemistry* **397,** 3173–8 (2010).

6. Woods, N., Muessig, A., Schmidt, M., Flygare, J., Olsson, K., Salmon, P., Trono, D., von Kalle, C., Karlsson, S. Lentiviral vector transduction of NOD / SCID repopulating cells results in multiple vector integrations per transduced cell : risk of insertional mutagenesis. *Blood* **101,** 1284–1289 (2003).

7. Seow, Y., Wood, M. J. Biological gene delivery vehicles: beyond viral vectors. *Molecular Therapy* **17,** 767–777 (2009).

8. Lowenstein, P. R., Mandel, R. J., Xiong, W., Kroeger, K., Maria, G., Immune Responses to Adenovirus and Adeno-Associated Vectors Used for Gene Therapy of Brain Diseases: The role of Immunological Synapses in Understanding the Cell Biology of Neuroimmune Interactions.*Current Gene Therapy* **7,** 347–360 (2008).

9. Monahan, P. E., Samulski, R. J. Adeno-associated virus vectors for gene therapy: more pros than cons? *Molecular Medicine Today* **6,** 433–440 (2000).

10. Prather, K. J., Sagar, S., Murphy, J., Chartrain, M. Industrial scale production of plasmid DNA for vaccine and gene therapy: plasmid design, production, and purification. *Enzyme Microbial Technol*ogy **33,** 865–883 (2003).

11. Simcikova, M., Prather, K. L. J., Prazeres, D. M. F., Monteiro, G. A. On the dual effect of glucose during production of pBAD/AraC-based minicircles. *Vaccine* **32,** 2843–6 (2014).

12. Herweijer, H., Wolff, J. a. Progress and prospects: naked DNA gene transfer and therapy. *Gene Therapy* **10,** 453–8 (2003).

13. Mehier-Humbert, S., Guy, R. H. Physical methods for gene transfer: improving the kinetics of gene

delivery into cells. *Advanced Drug Delivery Reviews* **57,** 733–53 (2005).

14. Suda, T., Liu, D. Hydrodynamic gene delivery: its principles and applications. *Molecular Therapy* **15,** 2063–2069 (2007).

15. Han, S. W., Nakamura, C., Obataya, I., Nakamura, N., Miyake, J. A molecular delivery system by using AFM and nanoneedle. *Biosensensors & Bioelectronics* **20,** 2120–5 (2005).

16. Han, S.-W., Nakamura, C., Kotobuki, N., Obataya, I., Ohgushi, H., Nagamune, T., Miyake, J. High-efficiency DNA injection into a single human mesenchymal stem cell using a nanoneedle and atomic force microscopy. *Nanomedicine* **4,** 215–25 (2008).

17. Haas, K., Sin, W., Javaherian, A., Li, Z., Cline, H. T. Single cell electroporation for gene transfer In vivo. *Neuron* **29,** 583–591 (2001).

18. Barrett, L. E.,Sul, J.-Y., Takano, H., Bockstaele, E.J.V., Haydon, P.G., Eberwine, J.H. Region-directed phototransfection reveals the functional significance of a dendritically synthesized transcription factor. *Nature Methods* **3,** 455–460 (2006).

19. Escoffre, J. M., Teissié, J., Rols, M. P. Gene transfer: How can the biological barriers be overcome? *Journal of Membrane Biology* **236,** 61–74 (2010).

20. Pannier, A. K., Shea, L. D. Controlled release systems for DNA delivery. *Molecular Therapy* **10,** 19–26 (2004).

21. Park, T. G., Jeong, J. H., Kim, S. W. Current status of polymeric gene delivery systems. *Advanced Drug Delivery Reviews* **58,** 467–86 (2006).

22. Lv, H., Zhang, S., Wang, B., Cui, S., Yan, J. Toxicity of cationic lipids and cationic polymers in gene delivery. *Journal of Controlled Release* **114,** 100–109 (2006).

23. Guang Liu, W., De Yao, K. Chitosan and its derivatives--a promising non-viral vector for gene transfection. *Journal of Controlled Release* **83,** 1–11 (2002).

24. Mintzer, M. A, Simanek, E. E. Nonviral Vectors for Gene Delivery. *Chemical Reviews* **109,** 259–302 (2008).

25. Dufes, C., Uchegbu, I. F.,Schätzlein, A. G. Dendrimers in gene delivery. *Advanced Drug Delivery Reviews* **57,** 2177–2202 (2005).

26. Sokolova, V. V, Radtke, I., Heumann, R., Epple, M. Effective transfection of cells with multi-shell calcium phosphate-DNA nanoparticles. *Biomaterials* **27,** 3147–53 (2006).

27. Felgner, P. L., Gadek, T.R., Holm, M., Roman, R., Chan, H.W., Wenz, M., Northrop, J.P., Ringold, G.M., Danielsen, M. Lipofection: a highly efficient, lipid-mediated DNA-transfection procedure.

Procedures of National Academy of Sciences of United States of America **84,** 7413–7417 (1987).

28. Rao, N. M., Gopal, V. Cell biological and biophysical aspects of lipid-mediated gene delivery. *Biosciences Reports* **26,** 301–324 (2006).

29. Tros de Ilarduya, C., Sun, Y., Düzgüneş, N. Gene delivery by lipoplexes and polyplexes. *European Journal of Pharmaceutical Sciences* **40,** 159–170 (2010).

30. Zhang, S., Xu, Y., Wang, B., Qiao, W., Liu, D., Li, Z. Cationic compounds used in lipoplexes and polyplexes for gene delivery. *Journal of Controlled Release* **100,** 165–180 (2004).

31. Rao, N. M. Cationic lipid-mediated nucleic acid delivery: beyond being cationic. *Chemistry and Physics of Lipids* **163,** 245–252 (2010).

32. Wasungu, L., Hoekstra, D. Cationic lipids, lipoplexes and intracellular delivery of genes. *Journal of Controled Release* **116,** 255–264 (2006).

33. Lima, M. C. P. De, Simões, S., Pires, P., Faneca, H., Düzgüneş, N. Cationic lipid – DNA complexes in gene delivery : from biophysics to biological applications. *Advanced Drug Delivery Reviews* **47,** 277–294 (2001).

34. Zhi, D., Zhang, S., Wang, B., Zhao, Y., Yang, B., Yu, S. Transfection efficiency of cationic lipids with different hydrophobic domains in gene delivery. *Bioconjugate Chemistry* **21,** 563–577 (2010).

35. Behr, J. P., Demeneix, B., Loeffler, J. P., Perez-Mutul, J. Efficient gene transfer into mammalian primary endocrine cells with lipopolyamine-coated DNA. *Procedures National Academy of Sciences of United States of America* **86,** 6982–6986 (1989).

36. Ferrari, M. E., Nguyen, C. M., Zelphati, O., Tsai, Y., Felgner, P. L. Analytical methods for the characterization of cationic lipid-nucleic acid complexes. *Human Gene Therapy* **9,** 341–351 (1998).

37. Felgner, J. H., Kumar, R., Sridhar, C. N., Wheeler, C.J., Tsai, Y.J., Border, R., Ramsey, P., Martin, M., Felgner, P.L. Enhanced gene delivery and mechanism studies with a novel series of cationic lipid formulations. *Journal of Biological Chemistry* **269,** 2550–2561 (1994).

38. Tang, F., Hughes, J. A. Synthesis of a single-tailed cationic lipid and investigation of its transfection. *Journal of Controlled Release* **62,** 345–358 (1999).

39. Mok, K. W., Cullis, P. R. Structural and fusogenic properties of cationic liposomes in the presence of plasmid DNA. *Biophysical Journal* **73,** 2534–2545 (1997).

40. Hui, S. W., Langner, M., Zhao, Y.L., Ross, P., Chan, K. The role of helper lipids in cationic liposome-mediated gene transfer. *Biophysical Journal* **71,** 590–599 (1996).

41. Liang, W., Lam, J. K. W. Endosomal Escape Pathways for Non-Viral Nucleic Acid Delivery Systems.

Molecular Regulation of Endocytosis 429–456 (2012).

42. Zuhorn, I. S.,Bakowsky, U., Polushkin, E., Visser, W.H., Stuart, M.C., Engberts, J.B., Hoekstra, D. Nonbilayer phase of lipoplex-membrane mixture determines endosomal escape of genetic cargo and transfection efficiency. *Molecular Therapy* **11,** 801–810 (2005).

43. Hirsch-Lerner, D., Zhang, M., Eliyahu, H., Ferrari, M.E., Wheeler, C.J., Barenholz, Y. Effect of 'helper lipid' on lipoplex electrostatics. *Biochimica et Biophysica Acta - Biomembr.* **1714,** 71–84 (2005).

44. Dua, J.S., Rana, A.C., Bhandari, A.K.. Liposome: methods of preparation and applications. *International Journal of Pharmaceutical Studies and Research* **III,** 7 (2012).

45. Madeira, C., Loura, L. M. S., Aires-Barros, M. R., Fedorov, A., Prieto, M. Characterization of DNA/lipid complexes by fluorescence resonance energy transfer. *Biophysical Journal* **85,** 3106–3119 (2003).

46. Schwendener, R. A., Ludewig, B., Cerny, A., Engler, O. Liposome-based vaccines. *Methods in Molecular Biology* **605,** 163–175 (2010).

47. Mansoori, M.A., Agrawal, S., Jawade, S., Khan, M.I. A review on liposome. *International Journal of Advanced Research in Pharmaceutical & Bio Sciences* **2,** 453–464 (2011).

48. Knight, J. D., Adami, R. C. Stabilization of DNA utilizing divalent cations and alcohol. *International Journal of Pharmaceutics* **264,** 15–24 (2003).

49. Ross, P. C., Hui, S. W. Lipoplex size is a major determinant of in vitro lipofection efficiency. *Gene Therapy* **6,** 651–659 (1999).

50. Zhang, X.-X., McIntosh, T. J., Grinstaff, M. W. Functional lipids and lipoplexes for improved gene delivery. *Biochimie* **94,** 42–58 (2012).

51. Safinya, C. R. Structures of lipid-DNA complexes: supramolecular assembly and gene delivery. *Current Opinion in Structural Biology* **11,** 440–8 (2001).

52. Lin, A. J., Slack, N.L., Ahmad, I., Koltover, I., George, C.X., Samuel, C.E., Safinya, C.R. Structure and structure-function studies of lipid/plasmid DNA complexes. *Journal of Drug Targeting* **8,** 13–27 (2000).

53. Stegmann, T., Legendre, J. Y. Gene transfer mediated by cationic lipids: lack of a correlation between lipid mixing and transfection. *Biochimica et Biophysa Acta* **1325,** 71–9 (1997).

54. Rejman, J., Bragonzi, A., Conese, M. Role of clathrin- and caveolae-mediated endocytosis in gene transfer mediated by lipo- and polyplexes. *Molecular Therapy* **12,** 468–474 (2005).

55. Mounkes, L. C., Zhong, W., Cipres-Palacin, G., Heath, T. D., Debs, R. J. Proteoglycans mediate

cationic liposome-DNA complex-based gene delivery in vitro and in vivo. *Journal of Biological Chemistry* **273,** 26164–26170 (1998).

56. Zabner, J., Fasbender, A. J., Moninger, T., Poellinger, K. A., Welsh, M. J. Cellular and molecular barriers to gene transfer by a cationic lipid. *Journal of Biological Chemistry* **270,** 18997–19007 (1995).

57. Zelphati, O., Szoka, F. C. Mechanism of oligonucleotide release from cationic liposomes. *Procedures of National Academy of Sciences of United States of America* **93,** 11493–11498 (1996).

58. Bloomfield, V. A. DNA Condensation by Multivalent Cations. *Biopolymers* **44,** 269–282 (1997).

59. Lam, a P., Dean, D. a. Progress and prospects: nuclear import of nonviral vectors. *Gene Ther*apy **17,** 439–47 (2010).

60. Cohen, R. N., van der Aa, M. a E. M., Macaraeg, N., Lee, A. P., Szoka, F. C. Quantification of plasmid DNA copies in the nucleus after lipoplex and polyplex transfection. *Journal of Controled Release* **135,** 166–174 (2009).

61. Sabatini, D. M. Reverse Transfection Method. International Publication Number WO 01/200015, filed 18 September 2000, published 22 March 2001 (2001).

62. Ziauddin, J., Sabatini, D. M. Microarrays of cells expressing defined cDNAs. *Nature* **411,** 107–110 (2001).

63. Fang, J., Zhu, Y.Y., Smiley, E., Bonadio, J., Rouleau, J.P. Goldstein, S.A., McCauley, l.K., Davidson, B.L., Roessler, B.J. Stimulation of new bone formation by direct transfer of osteogenic plasmid genes. *Procedures of National Academy of Sciences of Unied States of America* **93,** 5753–5758 (1996).

64. Shen, H., Goldberg, E., Saltzman, W. M. Gene expression and mucosal immune responses after vaginal DNA immunization in mice using a controlled delivery matrix. *Journal of Controlded Release* **86,** 339–348 (2003).

65. Kasahara, H., Tanaka, E., Fukuyama, N., Sato, E., Sakamoto, H., Tabata, Y., Ando, K., Iseki, H., Shinokazi Y., Kimura, K., Kuwabara, E., Koide, S., Nakazawa, H., Mori, H. Biodegradable gelatin hydrogel potentiates the angiogenic effect of fibroblast growth factor 4 plasmid in rabbit hindlimb ischemia. *Journal of the American College of Cardiology* **41,** 1056–1062 (2003).

66. Yoshikawa, T., Uchimura, E., Kishi, M., Funeriu. D.P., Miyake, M., Miyake, J.. Transfection microarray of human mesenchymal stem cells and on-chip siRNA gene knockdown. *Journal of Controlled Release* **96,** 227–232 (2004).

67. Reinisalo, M., Urtti, A., Honkakoski, P. Freeze-drying of cationic polymer DNA complexes enables their long-term storage and reverse transfection of post-mitotic cells. *Journal of Controlled Release* **110,** 437–443 (2006).

68. Uchimura, E., Yamada, S., Uebersax, L., Fujita, S., Miyake, M., Miyake, J. Method for reverse transfection using gold colloid as a nano-scaffold. *Journal of Bioscience and Bioengineering* **103,** 101–103 (2007).

69. Shen, H., Tan, J., Saltzman, W. M. Surface-mediated gene transfer from nanocomposites of controlled texture. *Nature Materials* **3,** 569–574 (2004).

70. Segura, T., Volk, M. J., Shea, L. D. Substrate-mediated DNA delivery: role of the cationic polymer structure and extent of modification. *Journal of Controlled Release* **93,** 69–84 (2003).

71. Kato, K., Umezawa, K., Funeriu, D. P., Miyake, M. Immobilized culture of nonadherent cells on an oleyl poly (ethylene glycol) ether-modified surface. *BioTechniques* **35,** 1–6 (2003).

72. Life Technologies. at <http://www.lifetechnologies.com/> (Acessed October2015)

73. Birkert, O., Haake, H.-M., Schütz, A., Mack, J., Brecht, A., Jung, G., Gauglitz, G. A streptavidin surface on planar glass substrates for the detection of biomolecular interaction. *Analytical Biochemistry* **282,** 200–208 (2000).

74. Yeo, D. S. Y., Panicker, R. C., Tan, L.-P., Yao, S. Q. Strategies for immobilization of biomolecules in a microarray. *Combinatorial Chemistry and High Throughput Screening* **7,** 213–21 (2004).

75. Escribá, P. V., González-Ros, J.M., Goñi, F.M., Kinnunem, P.K., Vigh, L., Sánchez-Magraner, L., Fernández, A.M., Busquets X., Horváth, I., Barceló-Coblijn, G. Membranes: A meeting point for lipids, proteins and therapies.. *Journal of Cellular and Molecular Medicine* **12,** 829–875 (2008).

76. Mathias, S., Peña, L. A., Kolesnick, R. N. Signal transduction of stress via ceramide. *The Biochemical Journal* **335,** 465–480 (1998).

77. Egner, A., Hell, S. W. Fluorescence microscopy with super-resolved optical sections. *Trends in Cell Biology* **15,** 207–215 (2005).

78. OLYMPUS. Laser Scanning Confocal Microscopy - Theory of Confocal Microscopy. at <http://www.olympusfluoview.com/theory/confocalintro.html> (Acessed January 2015)

79. Tauer, U. Dynamic Confocal Imaging of Living Brain Advantages and risks of multiphoton microscopy in physiology Experimental Physiology : Multiphoton microscopy is based on the simultaneous absorption of two photons emitted by a pulsed infrared Experimental Physiol. *Experiemental Physiology* **87.6,** 709–714 (2002).

80. Azevedo, A. M., Rosa, P.A., Ferreira, I.F., de Vries, J., Aires-Barros, M.R. Downstream processing of human antibodies integrating an extraction capture step and cation exchange chromatography. *Journal of Chromatography B: Analytical Technologies in the Biomedical and Life Sciences* **877,** 50–58 (2009).

81. Martins, S. A. M., Prazeres, D. M. F., Fonseca, L. P., Monteiro, G. A. Application of central composite design for DNA hybridization onto magnetic microparticles. *Analytical Biochemistry* **391,** 17–23 (2009).

82. Mandenius, C., Brundin, A. Review: biocatalysts and bioreactor design.Bioprocess optimization using design-of-experiments methodology. *Biotechnology Progress* **24,** 1191–1203 (2008).

83. Bezerra, M. A., Santelli, R. E., Oliveira, E. P., Villar, L. S., Escaleira, L. A. Response surface methodology (RSM) as a tool for optimization in analytical chemistry. *Talanta* **76,** 965–977 (2008).

84. Box, G. E. P., Wilson, K. B. On the Experimental Attainment of Optimum Conditions. *Journal of the Royal Statistical Society. Series B (Methodological)* **13,** 1–45 (1951).

85. Khan, M. K., Abert-Vian, M., Fabiano-Tixier, A.-S., Dangles, O., Chemat, F. Ultrasound-assisted extraction of polyphenols (flavanone glycosides) from orange (Citrus sinensis L.) peel. *Food Chemistry* **119,** 851–858 (2010).

86. Lebed, P. J., Potvin, S., Larivière, D., Dai, X. Optimization of solid phase extraction chromatography for the separation of Np from U and Pu using experimental design tools in complex matrices. *Analytical Methods* **6,** 139 (2014).

87. Carapuça, E., Azzoni, A. R., Prazeres, D. M. F., Monteiro, G.A., Mergulhão, F. J. M. Time-course determination of plasmid content in eukaryotic and prokaryotic cells using Real-Time PCR. *Moecular Biotechnol.* **37,** 120–126 (2007).

88. Azzoni, A. R., Ribeiro, S. C., Monteiro, G. A., Prazeres, D. M. F. The impact of polyadenilation signals on plasmid nuclease-resistance and transgene expression. *Journal of Gene Medicine* **9,** 392–402 (2007).

89. Diogo, M. M., Queiroz, J. A., Prazeres, D. M. F. Chromatography of plasmid DNA. in *Journal of Chromatography A* **1069,** 3–22 (2005).

90. Segura, T. Formulations and delivery Limitations of nucleic-acid-based therapies. In Gad, S.C. *Handbook of Pharmaceutical Biotechnology* 1013–1059 (John Wiley & Sons, Inc., 2007).

91. Caplen, N.J. Lipid gene transfer, a story of simplicity and complexity. In Xanthopoulos, K. G. *Gene Therapy* 185–204 (Springer, 1998).

92. Sarmento, M. J., Prieto, M., Fernandes, F. Reorganization of lipid domain distribution in giant unilamellar vesicles upon immobilization with different membrane tethers. *Biochimica et Biophysica Acta - Biomembranes* **1818,** 2605–2615 (2012).

93. Yang, Q., Liu, X. Y., Miyake, J., Toyotama, H. Self-assembly and immobilization of liposomes in fused-silica capillary by avidin-biotin binding. *Supramolecular Science* **5,** 769–772 (1998).

94. Bengali, Z., Rea, J. C., Shea, L. D. Gene expression and internalization following vector adsorption

to immobilized proteins: dependence on protein identity and density. *Journal of Gene Medicine* **9,** 668–678 (2007).

95. La Vega, J. De, Braak, B. Ter, Azzoni, A. R., Monteiro, G.A., Prazeres, D. M. F. Impact of plasmid quality on lipoplex-mediated transfection. *Journal of Pharmaceutical Science* **102,** 3932–3941 (2013).

96. Brunner, S., Sauer, T., Carotta, S., Cotton, M., Saltik, M., Wagner, E. Cell cycle dependence of gene transfer by lipoplex, polyplex and recombinant adenovirus. *Gene Therapy* **7,** 401–407 (2000).

97. Mortimer, I., Tam, p., MacLachlan, I., Graham, R.W., Saravolac, E.G., Joshi P.B. Cationic lipid-mediated transfection of cells in culture requires mitotic activity. *Gene Therapy* **6,** 403–411 (1999).

98. Tseng, W. C., Haselton, F. R., Giorgio, T. D. Mitosis enhances transgene expression of plasmid delivered by cationic liposomes. *Biochimica et Biophysica Acta - Gene Structure and Expression* **1445,** 53–64 (1999).

6. ANNEX

Table 6.1 Absolute values obtained in flow cytometry assays for the RSM assays. Four sets of replicates were performed. For a result to be statistically significant it must have 1000 events. Assays that didn't cross the 1000 limit weren't used and are marked as red. Maximum results (used to calculate the relative results) in each set are marked as green

	Set 1		Set 2		Set 3		Set 4	
	Events	% Cells Transfected	Events	% Cells Transfected	Events	% Cells Transfected	Events	% Cells Transfected
1	328	2.74	1179	2.63	7849	0.54	9855	1.98
2	45	11.11	436	4.82	8490	0.59	4580	2.6
3	1090	5.69	6065	2.26	8384	0.85	9813	1.79
4	1276	2.51	4667	0.94	8620	0.37	2589	1.85
5	0	0	3044	21.75	7929	4.28	4480	11.29
6	3741	1.9	4616	0.91	6583	0.52	3798	1.42
7	7937	2.86	6950	7.42	8886	1.91	2053	10.94
8	8118	1.36	6731	2.57	8509	1.32	7337	1.14
9	7905	2.2	5207	2.61	6826	2.64	4941	7.91
10	7222	2.15	5455	1.5	1114	1.26	6351	10.12
11	7350	0.98	5343	2.25	8971	1.37	4222	11.11
12	623	2.57	7890	1.13	9208	1.55	9884	12.77
13	2201	6	2829	19.44	7218	10.7	1730	0.52
14	7492	5.47	3040	17.93	8433	6.63	1025	63.32
15	7097	5.78	6330	10.6	7791	6.28	2795	1.61
16	7722	1.31	3993	3.93	8655	0.95	6500	35.45
17	7749	1.63	4275	3.72	7763	2.34	4535	9.9
18	5611	3.21	724	4.28	8448	4.56	2865	30.37
19	214	20.09	320	5	6055	2.99	7932	5.13
20	0	0	889	6.13	9356	2.88	4690	3.94
21	0	0	603	3.98	7839	1.89	4329	3.53
22	7860	1.21	3570	2.58	9726	2.48	9727	4.25
23	7610	3.55	1507	22.43	9351	2.94	5315	11.67
24	1135	2.64	314	10.19	7903	2.63	8014	3.08
25	7519	2.1	4722	5.39	6946	2.33	4834	11.13
26	0	0	6757	2.93	8684	1.77	6459	10.98
27	7927	2.07	7084	1.47	7678	4.17	8651	5.32
28	8247	2.69	5464	1.96	6876	2.24	9760	5.82
29	7836	2.64	7008	2.1	7176	1.51	9832	7.97
30	8003	3.59	**0**	0	8036	3.67	5360	7.31